HEAT CAPACITY MEASUREMENTS ON POLYETHYLENE IN THE TEMPERATURE RANGE OF 2.4 TO 300°K

JAMES EARL TUCKER

HEAT CAPACITY MEASUREMENTS ON POLYETHYLENE IN THE TEMPERATURE RANGE OF 2.4 TO 30°K

by

James Earl Tucker
Lieutenant Commander, U.S. Navy
B. S. Physics, Georgia Institute of Technology, 1956

Submitted in partial fulfillment
for the degree of

DOCTOR OF PHILOSOPHY IN PHYSICS

from the

UNITED STATES NAVAL POSTGRADUATE SCHOOL

May 1966

ABSTRACT

Specific heat measurements on three samples of polyethylene, differing only in density, were made in the temperature range of 2.4 to 30°K. A definite density dependence was noted for the specific heat in this temperature interval which allowed extrapolation of the data to completely crystalline and completely amorphous cases. At the lowest temperatures, the amorphous results were observed to display an "excess" heat capacity which could be accounted for by the occurance of a single delta function peak in the low frequency part of the vibrational spectrum. This excess did not appear in the completely crystalline extrapolated data, and the specific heat was found to be proportional to the cube of the temperature up to 9°K.

An attempt was made to compare the results with two theoretical models (Tarasov and Stockmayer-Hecht) with only fair agreement in one case, and none in the other. The agreement with previous experimental results is excellent if the density dependence and the excess heat capacity are considered.

TABLE OF CONTENTS

TABLE OF CONTENTS

LIST OF ILLUSTRATIONS

LIST OF TABLES

LIST OF ABBREVIATIONS

C, C_v	Heat capacity or specific heat
T	Temperature
h	Planck's constant (6.625×10^{-27} erg-sec)
k	Boltzman's constant (1.34×10^{-16} erg/^{o}K)
R	Universal gas constant (.08206 liter-atms/mole-^{o}K, 8.3143 j/mole-^{o}K)
^{o}K	Degree Kelvin

1. INTRODUCTION

General Remarks

The objective of the investigation which is the subject of this thesis was to determine the specific heat of polyethylene by direct calorimetric methods in the temperature range between 2.4 and 30°K. This study was prompted by some earlier results of low precision which indicated a rather sizeable density dependence of the specific heat in the low temperature range [34]. This observation was in contradiction to statements in the literature which denied such a dependence [52]. In addition, theoretical models had predicted an unusual behavior of the specific heat of fibrous solids, such as polyethylene, at low temperatures which had not been verified by previous measurements [19, 46, 47, 52]. It was hoped that these effects, if they were to occur, would be found in the range covered by the present experiment thus affording a comparison of the experimental results with the predictions. Further, it was desired to investigate the density dependence over a larger temperature range, and with more precision than that in the work noted above.

The unusual heat capacity behavior which had been predicted to take place is a consequence of the polyethylene molecules being long chains, and the forces along the chains being much larger than those between chains. This one dimensional characteristic gives rise to theoretical descriptions for the specific heat which differs from most other non-fibrous solids. The theoretical models based on this chain structure will be discussed later, as will the morphology of polyethylene. However, for now it should be noted that polyethylene is an example of a polymer which crystallizes partially, and thus is

neither completely crystalline nor completely amorphous. So, one parameter in any discussion of polyethylene must be of its crystallinity, which is directly related to its density. Making the assumption that polyethylene consists of two distinct forms, the crystalline and the amorphous, it is much simpler, for this discussion, to describe the specific heat of polyethylene in terms of the specific heat of these two idealized phases, i.e., the specific heat of any real sample can be expressed as an admixture of that of the two hypothetical ones. In order to accomplish this, the heat capacity of various samples differing in crystallinity (density) was determined so that extrapolation to the completely amorphous and crystalline cases could be made.

Heat capacity data for polyethylene is available from various sources in the temperature ranges from 1 to 5°K and from 20°K to its melting point (about 428°K). The results of this research will bridge the existing temperature gap and should be of interest for two reasons. First, since polyethylene is an archtype of the chain polymers, the behavior of its heat capacity over the entire temperature might be representative of polymers in general, and second, to allow a possible check on the aforementioned theoretical predictions.

Previous Measurements

Below 100°K there is not much experimental data on the specific heat of polyethylene. Above this temperature a considerable number of measurements have been made to determine the specific heat of the solid as it passes through the glass transition and the melting point. However these latter results are not germane to the present investigation.

The data for the temperature range below 5°K were available from two sources. Isaacs and Garland reported measurements on a single high density sample in the 1.8-5.3°K interval obtained by calorimetric methods [21]. The heat capacity of three samples of various densities was measured by indirect means in the range of from 1 to 4.5°K by Reese and Tucker [34]. The density dependence noted before is quite apparent when all four sets of measurements are compared [34]. It should be noted, however, that the data was analyzed assuming a cubic temperature dependence for the specific heat. This assumption is not verified by the present investigation, which shows a distinct non-cubic relation in this temperature region; however, the density dependence is valid.

Dainton, Hoare, Evans, and Melia give results for two samples in the range 20-300°K [13] . However no conclusions could be made about the density dependence, since the samples were very similar in density. The only other known source of specific heat data for polyethylene in this temperature range is the work of Sochava from 17 to 60°K [44]. The sample used by Sochava was not well characterized, the only information given being that it was a "typical commercial product". Thus there is no way to determine the density relationships in the higher temperature range above 20°K. Above 90°K there are more measurements but it is felt that this information was not of interest insofar as the present investigation is concerned.

Brief Description of Polyethylene

Chemically, polyethylene is one of the simplest forms of chain polymers, consisting only of CH_2 units. The bonding along the chain is covalent. The chain length can be varied during manufacture, but

in general it is quite long, on the order of 1000 units. In addition, side branches can and do form on the chain, and is also a parameter which can be varied according to the manufacturing process. These branches, which are short chain sections normally only 2-5 units long, join to the main chain by the substitution of a carbon-carbon bond for a carbon-hydrogen bond [31,38].

Polyethylene is one of the polymers which crystallizes partially in the bulk form. A necessary condition for crystallization is geometrical regularity of the molecular structure, which is fulfilled by the simple form of the polyethylene chain [10,31]. This regularity allows the chains to form ordered arrays, which are considered the crystalline state. However on the basis of single crystals grown from solutions, which are quite small, it appears that the crystals are lamella, approximately 100 Angstrom units thick, with the molecular chain axis being perpendicular to the face [23,35]. Whether this crystalline form is the same in the bulk is not known conclusively [31]. However, it is well established that the crystalline part of polyethylene is composed of clusters of spherulites [31].

The most important factor inhibiting crystal formation is branching. This is evidenced by the fact that highly branched polyethylene displays relatively low crystalline content [45]. This is quite reasonable since the regularity of the structure is broken at the branch points, thereby producing discontinuities or distortions in the crystal.

If the chain is not in the well ordered array of the crystalline state, it is in some metastable position, intertwined and twisted around other chains. The complexity of the non-crystalline form makes

description very difficult. However, it sufficient for this discussion to characterize the non-crystalline part of the polyethylene as the amorphous regions.

Since in the crystalline part of the polyethylene the molecules are more closely packed than in the amorphous, a higher density is found for the crystalline phase than for the amorphous [15]. In fact if the density, ρ, of a particular sample is known, its weight percent crystallinity, X, can be calculated from the relation,

$$X = \frac{\rho_c}{\rho}\left(\frac{\rho - \rho_A}{\rho_c - \rho_A}\right), \tag{1.1}$$

where ρ_c and ρ_A refer to the densities of the crystalline and amorphous parts which are abtained by indirect methods [15]. The crystallinities of bulk polyethylene vary in general between 35 and 95%.

Heat Capacity Models

The specific heat of a solid can be calculated if the temperature dependence of its internal energy, U, is known. This follows from the definition

$$C_v = \frac{\partial U}{\partial T}\Big)_v. \tag{1.2}$$

If the internal energy's temperature dependence is due to vibrations of the constituent parts of the solid about their equilibrium positions, the total energy of oscillation over the whole range of the vibrational spectrum is,

$$U = \int_0^\infty g(\nu)\, E_p(\nu, T)\, d\nu, \tag{1.3}$$

where $E_p(\nu, T) = h\nu/(e^{h\nu/kT} - 1)$ is the average energy of a Planck oscillator with vibrational frequency ν, and $g(\nu)$ is the distribution function for the eigenfrequencies of elastic vibrations of the solid, which is called the frequency spectrum [14]. If there are N mass points in the solid, then there can be only 3N normal modes of vibration, assuming that the temperatures are sufficiently low that possible internal motion of the mass units can be neglected (the optical modes of vibration). This sets the restriction

$$3N = \int_0^\infty g(\nu)\,d\nu \quad . \tag{1.4}$$

Rigorous treatment shows that the upper limits in the integrals in equations 1.3 and 1.4 can be replaced by a maximum or cut-off frequency ν_m [50]. Hence if $g(\nu)$ is known, ν_m can be determined from equation 1.4.

This cut-off frequency can be interpreted as the frequency at which two neighboring mass units differ in phase by 180°. It should also be noted that ν_m is related to the forces acting between the neighbors, that is, greater forces imply larger cut-off frequencies, assuming particles of equal mass [14].

The central problem in the calculation of the internal energy of a system, and therefore its specific heat, is to find the frequency spectrum $g(\nu)$. This is in general extremely difficult. Therefore, several approximation methods have been employed for solids. One of the most successful approximations is the Debye model.

The Debye approximations are that the frequency spectrum is that calculated assuming the solid is an isotropic continuum, subject only to the condition stated above concerning the cut-off frequency, and that there is a linear relation between the frequency and the wave

number, i.e., that there is no dispersion. These approximations can be expected to hold for long wavelengths (low temperature) [50]. Debye theory than predicts a frequency distribution given by

$$1.5 \qquad g(\nu)d\nu = \begin{cases} 9N \dfrac{\nu^2 d\nu}{\nu_m^3} & \nu < \nu_m \\ 0 & \nu_m < \nu . \end{cases}$$

Using this in equations 1.2, 1.3 and 1.4 leads to the familiar Debye equation for the specific heat,

$$1.6 \qquad C_v = 3R\, D_3\left(\frac{\theta_D}{T}\right)$$

where $D_3\left(\frac{\theta_D}{T}\right) = 12\left(\frac{T}{\theta_D}\right)^3 \int_0^{\theta_D/T} \frac{x^3 dx}{e^x - 1} - 3\, \frac{\theta_D/T}{e^{\theta_D/T} - 1}$

and $\theta_D = \frac{h\nu_m}{k}$ is a characteristic temperature of the material called the Debye temperature. For very low temperatures, $\frac{T}{\theta_D} << \frac{1}{30}$, equation 1.6 reduces to,

$$1.7 \qquad C_v = 3R\, \frac{4\pi^4}{5} \left(\frac{T}{\theta_D}\right)^3 \qquad T \to 0$$

and for very high temperatures,

$$1.8 \qquad C_v = 3R \qquad T \to \infty .$$

This last result is the same as is predicted classically using the equipartition of energy [24].

As a logical extention of this model, it is more reasonable to assume that there exists a cutoff wavelength, rather than a maximum frequency. Since it is known that for all solids the velocity of sound is dependent of the direction of propagation, the cut-off frequency will also be different for the different modes and directions [43]. Recognizing this, equations 1.5 and 1.6 become,

1.9 $$g(\nu)d\nu = \begin{cases} 3N\left(\frac{2\nu^2}{\nu_t^3} + \frac{\nu^2}{\nu_l^3}\right)d\nu & \nu < \nu_t \\ 3N\frac{\nu^2 d\nu}{\nu_l^3} & \nu_t < \nu < \nu_l \\ 0 & \nu_l < \nu \end{cases}$$

1.10 $$C_v = R\left[2D_3\left(\frac{\theta_t}{T}\right) + D_3\left(\frac{\theta_l}{T}\right)\right]$$

where the subscripts refer to the transverse and longitudinal modes, and the ν_m's are directly related to the average sound velocities in these two modes. It should be noted that this modification preserves the T^3 dependence of the specific heat at the lowest temperatures.

Polymers differ from most other solids in the sense that they are essentially one dimensional in nature, because the forces acting along the chains are much greater than those between chains. If a Debye-type analysis is made for a one dimensional system, in a manner completely analogous to the preceeding, one obtains the following results [47];

1.11 $$g'(\nu)d\nu = \begin{cases} 3N\frac{d\nu}{\nu_m'} & \nu < \nu_m' \\ 0 & \nu_m' < \nu \end{cases}$$

1.12 $$C_v = 3R\,D_1\left(\frac{\theta_1}{T}\right)$$

where $$D_1\left(\frac{\theta_1}{T}\right) = 2\left(\frac{T}{\theta_1}\right)\int_0^{\theta_1/T}\frac{x\,dx}{e^x - 1} - \frac{\theta_1/T}{e^{\theta_1/T} - 1}$$

and $$\theta_1 = \frac{h\nu_m'}{k}.$$

The model employed above describes non-interacting chains, so is not of direct interest in this discussion. However, if the chains are intertwined and linked with one another, as in a chain polymer

such as polyethylene, there will be both the three dimensional and one dimensional continua existing together. This is the basis of a model due to Tarasov [47] . Since the forces acting along the chain are much greater than those between chains, it is expected that the maximum frequency for the one dimensional part of the model will be greater than that for the three dimensional part. Tarasov therefore predicted that there would exist two frequency spectra such that,

$$3N = \int_0^{\nu_3} g_3(\nu)d\nu + \int_{\nu_3}^{\nu_1} g_1(\nu)d\nu \qquad 1.13$$

where the subscripts refer to the one and three dimensional quantities. Using the Debye assumptions, frequency distributions can be found. However, the separation into transverse and longitudinal parts is again applicable, as it was above. For the remainder of this derivation only the longitudinal part will be considered, and the transverse contributions put in at the end by analogy with the Debye case. Therefore equation 1.13 becomes,

$$N = \int_0^{\nu_3^{\ell}} g_3^{\ell}(\nu)d\nu + \int_{\nu_3^{\ell}}^{\nu_1^{\ell}} g_1^{\ell}(\nu)d\nu \qquad 1.14$$

for the longitudinal mode only (denoted by the superscript ℓ). This equation can be rewritten as

$$N = N_{30} + N_{13} \qquad 1.15$$

where N_{30} and N_{13} refer to the first and second integrals above. The distribution of the modes are, for N_{13}

$$g_1^{\ell}(\nu)d\nu = \begin{cases} N_{13}\dfrac{d\nu}{\nu_1^{\ell}-\nu_3^{\ell}} & \nu_3^{\ell} < \nu < \nu_1^{\ell} \\ 0 & \nu_1^{\ell} < \nu\,;\ \nu < \nu_3^{\ell} \end{cases} \qquad 1.16$$

and, for N_{30},

1.17 $$g_3^l(\nu)d\nu = \begin{cases} 3N_3 \dfrac{\nu^2 d\nu}{(\nu_3^l)^3} & \nu < \nu_3^l \\ 0 & \nu_3^l < \nu. \end{cases}$$

If these spectra are the correct ones, the heat capacity is given by the resulting Tarasov equation,

1.18 $$C_v^l = R\left\{D_1\left(\frac{\theta_{1L}}{T}\right) - \frac{\theta_{3L}}{\theta_{1L}}\left[D_1\left(\frac{\theta_{3L}}{T}\right) - D_3\left(\frac{\theta_{3L}}{T}\right)\right]\right\}$$

for the longitudinal mode, where θ_{1L}, θ_{3L} are related to ν_1^l, ν_3^l and the other symbols have been previously defined. Inclusion of the transverse modes then yields the complete Tarasov relation,

1.19 $$C_v = C_v^l + 2C_v^t.$$

In the two temperature extremes, equation 1.19 reduces to

1.20 $$C_v = 3R\,\frac{4\pi^4}{5}\,T^3\left[\frac{1}{3}\left(\frac{2}{\theta_{1T}\,\theta_{3T}^2} + \frac{1}{\theta_{1L}\,\theta_{3L}^2}\right)\right] \qquad T \to 0$$

1.21 $$C_v = 3R \qquad T \to \infty.$$

Between these extremes, there will be a region for which,

1.22 $$C_v = 3R\,\frac{\pi^2}{3}\left[\frac{1}{3}\left(\frac{2}{\theta_{1T}} + \frac{1}{\theta_{1L}}\right)\right] \qquad T,\ \theta_3 \ll \theta_1.$$

No continuum model should be expected to explain the specific heat in the presence of dispersion, which will take place in any real lattice. In order to calculate the density of states in the vibrational spectrum correctly, the effects of all of the forces acting between the mass units must be included. In practice this is not feasible. As a result, the usual method of approach is to make realistic estimates of the strength of the forces, and drop all but the

dominate ones from the calculations. Blackman, and many others since, have achieved a certain amount of success along these lines; the degree of success depending on the validity of the assumptions about the relative strength of the forces, and the number of forces included in the calculations [6,7,16,28]. This type of analysis, since it employs the discrete nature of the solid, should be more complete than the continuum treatment, if the correct parameters are used. There is however one feature of the lattice dynamics calculations which is the same as that obtained by the continuum assumptions: the heat capacity at the lowest temperatures should be proportional to the cube of the absolute temperature.

For crystalline chain polymers an attempt has been made to obtain the vibrational spectrum using lattice dynamics by Stockmayer and Hecht whose work was greatly extended by Genensky and Newell [19,46]. This analysis is based on the consideration that there are strong forces along the chains and weaker ones between them. The frequency spectrum deduced was quite complicated, but has certain characteristics which are predicted to be characteristic of the heat capacity of fibrous solids in the crystalline form, and thus should be applicable to crystalline polyethylene. These predictions include, (where C_1 now refers to the specific heat contribution from the interchain interaction, and C_3 to that along the chain) [19]

1.23 $$C_v = \frac{2C_1 + C_3}{3}$$

and

1.24 $$C_1 \propto T^3 \qquad T \ll \frac{\alpha}{2\sqrt{K}} T_m$$

1.25 $$C_1 \propto T^{5/2} \qquad \frac{\alpha}{2\sqrt{K}} T_m \ll T \ll \sqrt{\alpha}\, T_m$$

1.26 $C_1 \propto T^{1/2}$ $\sqrt{\alpha}\, T_m \ll T \ll T_m$

1.27 $C_3 \propto T^3$ $T \ll \sqrt{\alpha}\, T_m$

1.28 $C_3 \propto T$ $2\sqrt{\alpha}\, T_m \ll T \ll T_m$

where T_m is proportional to the maximum vibrational frequency ν_m, α is related to the nearest neighbor forces, and K to the forces which oppose the bending of the chain. The approximations are,

1.29 $\beta/\alpha > 25$, $\beta/K > 10$, $\gamma \sim \alpha$

where β is related to the force constant along the chain, and γ is related to the second nearest neighbor forces. Using these relations temperature regions are predicted for which the heat capacity is at first (lowest temperatures) proportional to the cube of the temperature, then changes to a T^b dependence, where b lies between 2.5 and 3, than b decreases to approximately .8 for T about one half T_m.

To complete this brief treatment of specific heat models which might be applicable to polyethylene, a related phenomenon, which appears in the low temperature heat capacity of some amorphous solids, must be mentioned. If the heat capacity of these substances is measured calorimetrically at low temperatures, an "excess" specific heat is observed. To understand the term excess one should refer to equation 1.7 which can be rewritten as [24],

1.30 $$C_v = \frac{16\pi^5}{5} \frac{k^4}{h^3} V \frac{T^3}{v^3}$$

where V is the volume of the sample, and v is the velocity of sound at these temperatures, which can be interpeted as,

1.31 $$\frac{1}{v^3} = \frac{1}{3}\left(\frac{1}{v_l^3} + \frac{2}{v_t^3}\right).$$

Therefore sound velocity measurements should yield the same value for C/T^3 as those obtained from direct calorimetric methods. However, it has been found experimentally that for some amorphous substances, such as vitreous germanium, vitreous silica, and glycerol glass, the calorimetric results are much greater than those given by the acoustic methods and are not T^3 dependent [4,12,17].

The explanation for this anomolous effect is that at low temperatures there may be modes excited which are not measured by the acoustic methods. Since the mechanical sound measurements are concerned with the averaged (in the sense that the measurements must be macroscopic) elastic forces between the particles making up the solid, if there are low frequency modes which do not enter into these elastic vibrations, then the calorimetric measurements should be higher than predicted by equation 1.30. To explain the existence of these extra modes, Rosenstock has suggested that in disordered lattices, such as the amorphous solids, microscopic holes exist which may contain a particle which is bound in only one or two directions [39,40]. These loosely bound mass units can be likened to particles free to vibrate within a definite volume (the hole), and could thereby account for the low frequency non-acoustic modes. However, there are other hypotheses which attempt to explain the modes as being due to other phenomena such as non-symmetric lattice sites or distorted bonds [3,27]. In any case, the origin of these low frequency modes is not clear at this time. In the case of the examples cited above it has been possible to empirically describe the low temperature departure of the

specific heat from the T^3 relation by adding a term (or terms) proportional to the Einstein specific heat to equation 1.30 [2,4,17] . This implicitly implys that some of the vibrating units do not contribute to the acoustic modes and are accounted for in the total specific heat by an expression such as,

$$1.32 \qquad C_{Ex} = 3N_E h E\left(\frac{\theta_E}{T}\right)$$

where $\theta_E = \frac{h\nu_E}{h}$, $E\left(\frac{\theta_E}{T}\right) = \left(\frac{\theta_E/T}{e^{\theta E/T}-1}\right)^2 e^{\theta E/T}$,

ν_E is the excitation frequency for these modes, and N_E is the number of vibrators involved [24]. Adding a term such as this to equation 1.7 or 1.30 results in

$$1.33 \qquad C_v = AT^3 + BE\left(\frac{\theta_E}{T}\right)$$

where A and B are constants. Since the specific heat is no longer proportional to the cube of the temperature, a plot of the C/T^3 versus temperature will demonstrate the presence of the excess heat capacity.

2. EXPERIMENTAL DETAILS

Introduction

In all calorimetric investigations it is necessary to know two quantities; the temperature of the sample and the acount of heat added to it. In this experiment, meeting the former requirement was the more difficult.

The temperature determination must be made quickly and accurately. Since resistance thermometry fulfills these requirements, doped germanium resistors were selected as thermometers. These were chosen rather than carbon resistors since germanium resistors are reputed to maintain their resistance-temperature relationship even after a

large number of cyclings between room temperatures and liquid helium temperature [18,25] . Other experimenters have found that this is not true for carbon resistors, so that they must be recalibrated after each temperature cycling [18] . The need for recalibration would greatly complicate the experiment thus making the choice of germanium resistors an easy one.

Since the temperature range covered by this investigation was from about 2 to 30°K, doped germanium resistors (Minneapolis-Honeywell, models 2401 and 3401) were selected which had sufficiently high sensitivity, and yet, for the above temperatures, had resistance values within the range of ordinary laboratory resistance measuring devices. Once the resistors were chosen the most important task was to find the relation between the resistance and the absolute temperature. The discussion of the calibration procedures is the subject of Appendix A.

Having insured that a quick and accurate determination of the sample temperature and its changes could be made, attention was directed to the second requirement. Adding heat electrically to a resistance element in thermal contact with the sample provides a simple and accurate method of deliberately raising the sample's temperature. However great care must be taken to insure that this energy goes solely to the sample, and that it is the only source of heat input. To this end, an adiabatic calorimeter was constructed in which the sample could be suspended in vaccuo by high thermal resistance mountings from a heat shield, which completely surrounded the sample and was held at the same temperature. The design and construction of this calorimeter will be discussed in a subsequent section.

Sample Preparation

The heat capacity of three polyethylene samples of various densities were to be measured. Two of the samples were Marlex, manufactured by Phillips Petrolium Company, and were received in the form of extruded cylindrical pellets approximately 3 mm. in diameter and length. One of the samples, Marlex II, had branching introduced to impede crystallization. The third sample, a typical commercial low density polyethylene, was a 1" round bar. The samples are referred to as Marlex I, Marlex II, and Low Density in the remainder of this thesis.

An important consideration in the preparation of the samples was that the time interval between the application of heat and the achievement of thermal equilibrium be as short as possible so as to minimize errors due to heat leaks into or out of the sample. The low thermal conductivity of polyethylene at low temperatures makes this a difficult problem [34]. Because of the calorimeter design, the samples were to be cast into 9/16" rods about 6 cm. in length. If such a polyethylene rod were heated from the center, it was estimated that it would require times of about 100 seconds to achieve thermal equilibrium at $5^{o}K$ and nearly 1 1/2 hours at $30^{o}K$. Such comparatively long thermal relaxation times would undoubtedly introduce serious errors in the determination of the amount of heat added to the sample unless exceptional precautions in the control of the temperature of the adiabatic shield were taken, in addition to making the experiment extremely tedious to perform. Thus considerable effort was expended to prepare samples with shorter thermal equilibrium times. The method chosen was in inbed within the sample 99.999% pure copper wires such

that the wires were no farther than .3 cm. apart. In addition the sample was wrapped in a copper foil. The heat could thus be distributed throughout the sample by means of low thermal resistance copper paths. This was expected to greatly reduce the thermal relaxation times estimated above. The success of this method is seen by the fact that the time required during the actual experiment to achieve thermal equilibrium was never more than about 12 minutes at the highest temperatures.

Introduction of the wires into the sample in a uniform fashion presented a considerable problem. The following system was eventually evolved. The pellets (or in the case of the low density sample, the shavings obtained from turning the bar on a lathe) were first cast into small rods of 1/4" and 3/16", and wrapped with 30" of the copper wire. The rods were compactly assembled within a 9/16" mold, and additional wires inserted into the resulting gaps. The sample was then cast at 155°C under 900 PSI for 16 hours, and then allowed to cool to room temperature (about 12 hours).

The extra material added to the samples was to be considered part of the calorimeter's sample holder. It consisted of 30' of .0051" diameter drawn copper wire, .001" thick copper foil 5.580 by 5.035 cm., and .08 grams of G.E. 7031 varnish.

The polyethylene density was determined by measuring the density of the entire sample and correcting for the copper wire which was introduced. The crystallinity of each sample was then calculated by use of equation 1.1 with the values

2.1 $\rho_A = .854$ gm/cm^3

2.2 $\rho_C = .999$ gm/cm^3

where the ρ_A and ρ_c refer to pure amorphous and crystalline polyethylene densities [9,36]. It must be noted here that the densities given above are not the only ones available. For the amorphous case there is fair agreement in the literature that .85 is a good average, but more attention must be given to the crystalline density [15]. For this case, the density has been measured by X-ray methods to be as high as 1.014 gm/cm^3 and as low as .964 gm/cm^3 depending on the amount of branching present [49]. Furthermore voids or free volume in the spherulitic crystalline form of bulk polyethylene could reduce the higher figure noted above even in the absence of branching [10,11]. These considerations will be referred to again when the error of the experiment is discussed. The measured densities and calculated crystallinities are given in the table below, where the error indicated in the latter quantity is that due to the uncertainty in the density measurement only.

TABLE I

Densities and crystallinities of the samples.

	Density	% Crystallinity
Marlex I	.973 ± .002 gm/cm^3	84.1 ± 1.5%
Marlex II	.958 ± .002	74.5 ± 1.6
Low Density	.915 ± .002	45.9 ± 2.5

Calorimeter Design and Construction

In order to accurately measure heat capacities, the sample must be thermally isolated to insure that the noted temperature differences of the sample are due entirely to the measured heat input. To accomplish this, it is necessary to remove all conduction and radiation paths to and from the sample. The method employed here was to enclose

the sample in a shield which is kept at the same temperature as the sample, but insulated from it.

In this experiment the heat capacity would be measured at various temperatures above the temperature of a liquid helium bath by successive applications of heat to the sample. Hence the shield could not be in good thermal contact with the bath. This thermal isolation was accomplished by suspending the shield inside of a vacuum container which was in turn in contact with the bath. A can type adiabatic shield was made from a copper 2" tube, 3" long, threaded at the top to mate with its lid. The lid was soldered to a 3/8" stainless tube (.01" wall thickness), which connected to a suitable vacuum container. The tube then extended out of the cryostat to peripheral vacuum equipment and served as the pumping line and electrical lead housing. The shield also had provisions for receiving a resistor which would sense the shield's temperature.

There would be a heat leak from the shield to the vacuum container through the support, but this was compensated for by means of an electrical heater on the shield. In addition this heater was used to raise the shield's temperature to that of the sample. Seventeen feet of .002" manganin wire, coiled and glued with G.E. 7031 varnish to the top of the shield, served as the shield heater.

The sample holder, in addition to holding the 9/16" sample, was used to mount the sample heater, temperature sensing resistor, and a receptacle which would be the contact point for the thermal switch (to be discussed later). A copper ring with the necessary provisions was constructed for this purpose. When heat capacity measurements were made, the measured values would be the total of the sample plus

the addenda (the holder, heater, thermometer, etc.). Although the latter's heat capacity would be determined experimentally and subtracted from the total, it was still desirable to keep it as small as possible. Based on the size of the calorimeter, it was determined that a sample of 10 cm^3 could be accommodated. With a sample of this size it was estimated (correctly, as was determined later) that the heat capacity of the addenda would amount to less than 10% of the total, which was deemed acceptable.

The sample heater, which consisted of 15" of .002" manganin wire (100 ohms), was wound around the thermometer receptacle. A four wire connection was made to the heater, and the wires were thermally grounded to the adiabatic shield. The power was measured potentiometrically using a Leeds and Northrup K-3 potentiometer. A Varian model 501A time mark generator, used in conjunction with a Hewlett-Packard model 521C electronic counter, determined the heating times (the timer was later changed to an Anadex model CF-200R counter-timer) and was triggered by the sample heater switch.

It would be impossible, regardless of the care taken, to insure that the shield would be at exactly the same temperature as the sample at all times. However, if the shield were thermally isolated from the sample, small temperature differences could be tolerated. Based on this the sample holder was suspended within the shield by 6 nylon threads, approximately .12 mm. in diameter, and a minimum of 1.9 cm. in length. Assuming a maximum of $.5^{o}$ temperature difference between the shield and the sample, the heat leak through these supports would be on the order of 10^{-5} mj/sec which, for equilibrium times of less than an hour, could be neglected (radiation losses are of the same order of magnitude).

When the calorimeter was initially cooled, or when cooling back to the bath temperature after a series of measurements, a method had to be incorporated in the design to cool the isolated sample in a reasonable length of time. For this reason a mechanical switching device was constructed. This was chosen over the use of exchange gas in the vacuum spaces, since the latter method has been shown to have quite long recovery times and has attendent gas absorption problems [29]. The switch consisted of a brass finger which would make contact with a receptacle on the sample holder. The finger was soldered to a brass rod which extended out of the vacuum container into the liquid helium bath through a nickel bellows and from there out of the cryostat. The finger could be raised and lowered manually so as to make thermal and mechanical contact with the holder whenever it was required. The original design was modified after an initial trial by tinning the brass finger and its mating receptacle with metallic indium, for better thermal contact. In addition a brass leaf was added which would make contact with the adiabatic shield when the thermal switch was closed in order to cool the entire calorimeter simultaneously.

The two thermometers (resistors) were attached to the shield and the sample. Three wire connections, which were thermally anchored to the shield, were made to each resistor. The resistance measuring equipment was identical to that used by Reese and Tucker and will not be discussed here [34].

The completed calorimeter is shown in figure 1.

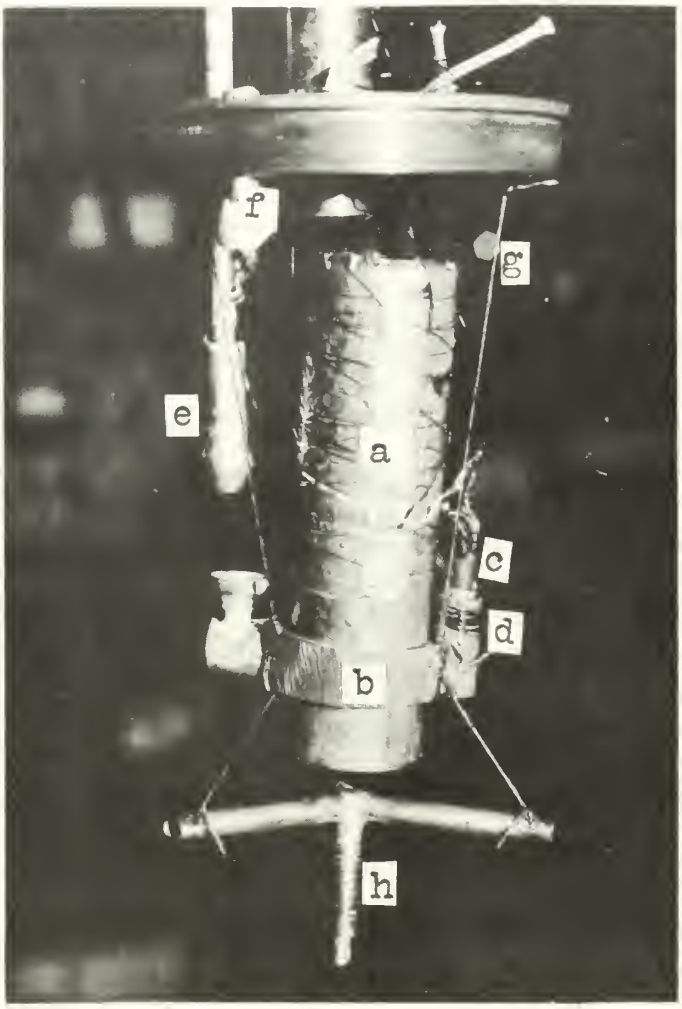

Figure 1. Calorimeter with sample in place.

a. Sample
b. Sample holder
c. Sample thermometer
d. Sample heater
e. Thermal switch
f. Shield thermometer
g. Nylon support
h. Anchor

Measurement Procedures

In preparation for the heat capacity measurements, the sample was placed in the calorimeter and cooled to the desired initial temperature with the thermal switch closed. When the thermometers indicated that the sample and shield were at the liquid helium bath temperature, the thermal switch was then opened. This set up a small amount of frictional heating as the contact was broken, but within 30 minutes the system would again be in equilibrium.

The sample was then heated by applying electrical power to the sample heater in amounts which would raise the temperature of the sample in 5% increments of its average temperature. The power was recorded at each temperature step as well as the initial and final readings of the time and the thermometers. The heating times were kept between 20 and 60 seconds, which required that the power be increased every four to six measurements. When the desired final temperature was reached, the thermal switch was again closed, the sample cooled, and the procedure repeated.

While the heat was being supplied to the sample, the adiabatic shield was also heated by means of its heater. This required care since, as previously mentioned, it was highly desirable that the shield and the sample be at the same temperature. After several trials, however, certain regularities in the amount of heat needed for the shield at various temperatures became evident, and the desired result was obtained. It is felt that there never existed more than a one percent temperature difference between the two thermometers while actual measurements were being taken, and for the bulk of the runs, the difference was considerably less.

Due to the close proximity of sample thermometer to the heater, while the power was being supplied the temperature would be observed to overshoot the desired value, and, when the power was removed, drop back exponentially. The time required for the sample to reach equilibrium was from 2 seconds to about 12 minutes as the temperature was increased from its lowest value to its highest. These times were not considered excessive, except at the highest temperatures when the shield might tend to drift while equilibrium was being established. This drifting was countered by monitoring both thermometers and keeping the shield at the desired temperature by removing or increasing the shield power.

The heat capacity of the samples was determined by five separate sets of measurements. The first three covered the range of 4.5 to 30°K, one series for each of the three samples. The other two were for the temperature interval 2.4 to about 8°K for the Marlex I and Low Density samples only. For each set of measurements the aforementioned temperature ranges were covered three times.

Since the measured heat capacities were the sum of those of the sample and the addenda, the latter was measured in two separate experiments, for the temperature ranges of 4.5 to 30°K and 2.4 to 8°K, so that its contribution could be subtracted from the total. In each of the experiments, the addenda heat capacity was measured four times over the covered range. The procedures were identical to those described above except due to the reduced mass, the amount of heat required and the equilibrium times were both substantially decreased.

3. RESULTS OF THE EXPERIMENT

Data Reduction

When the experimental measurements of the heat capacity were

made, the data consisted of the power reading, the elapsed time interval during which the power was applied, and the initial and final temperatures as indicated by resistance values. The heat capacity can then be calculated from,

$$3.1 \qquad C = \frac{\text{Power X Elapsed Time}}{T_{Final} - T_{Initial}} .$$

Due to the complexity of the resistance-temperature relation (Appendix A), the calculations were performed by the CDC 1604 digital computer.

All of the data were reduced to heat capacities, and of the ones which displayed large deviations, only those attributable to obvious blunders in data recording were rejected.

Since the heat capacities measurements for each sample represented the total of the sample plus the addenda, the latter's contribution had to be taken into account and corrected for. As mentioned before, measurements of the heat capacity of the addenda were performed. These heat capacities were for discrete, random temperatures and, as such, were not useful for the adjustment which was to be made. Therefore the data were best fitted, in the least squared sense, by the computer to a continuous heat capacity-temperature relation of the form,

$$3.2 \qquad C = \sum_{i=1}^{7} A_i T^{i-1} .$$

With this relationship the total heat capacity for each sample could be corrected so that the specific heat of the sample alone could be determined. These calculations were also performed by the computer and the resulting heat capacity data were again fitted to

equation 3.2. The specific heat was obtained by dividing the heat capacity by the mass of the sample.

The measured specific heat for each sample is found in Appendix C, and the parameters of equation 3.2 for the samples and the addenda in Appendix E. The smoothed results from the fitted curve are shown in Appendix D, and a specific heat-temperature graph is displayed in figure 2 where the difference between the smoothed curve and the actual data points is too small to be shown.

The temperature range, total number of data points, and the per cent RMS deviation of the actual data from the smooth curve are presented in Table II.

Table II

Temperature range, amount of data, and RMS fit of the data to a smoothed curve for each of the samples and the addenda.

	Temperature range	Number of data points	%RMS deviation
Addenda	2.4 - 30°K	218	1.70%
Marlex I	2.4 - 30	161	1.52
Marlex II	4.5 - 30	117	1.01
Low Density	2.4 - 30	158	1.09

Extrapolation to 100% and 0% Crystallinity

As mentioned in the first chapter, the specific heat of any polyethylene sample might best be expressed as admixture of the specific heats of the completely amorphous and completely crystalline phases. As suggested by the earlier low precision work of Reese and Tucker, and very well substantiated by the present investigation, the relation is linear [34]. That is

$$3.3 \qquad C = X C_{100} + (1-X) C_0$$

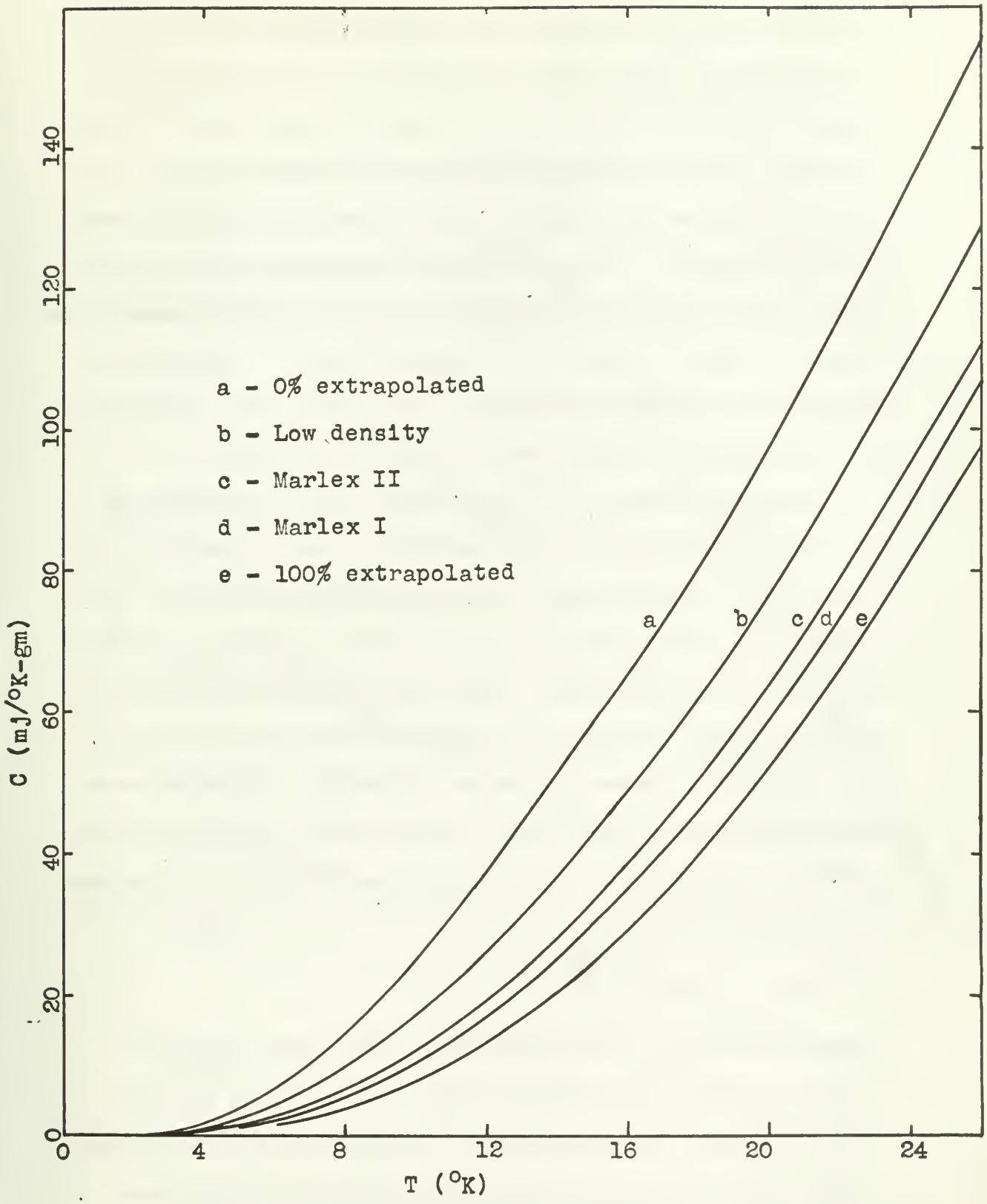

Figure 2. Specific heat versus temperature.

where the C's on the right side refer to hypothetical values for the specific heat of crystalline and amorphous polyethylene. This linearity is reasonable if one considers that it is possible (in theory) to break a sample up into many very small macroscopic volumes, each of which is either entirely amorphous or crystalline (if the boundaries are neglected). The two idealized polyethylenes should have different values for the specific heat at any particular low temperature, since the amorphous state should be characterized by a set of parameters which will differ from those of the crystalline state inasmuch as the interchain binding scheme is completely different.

Using this assumption, the heat capacities for the three samples, divided by the cube of the temperature, were plotted as a function of crystallinity for various temperatures (Figure 3). The linearity is quite apparent, and on the basis of this, it is felt that equation 3.3 is indeed valid. Using this linear relationship one can perform a simple extrapolation to obtain values for the specific heat as a function of temperature for the hypothetical 100% and 0% cases. However, rather than use the C/T^3 relation, which is shown for descriptive purposes only, the computer was used to perform the extrapolation from the equation

$$C = m X + b \qquad 3.4$$

where m and b were determined from the experimental (smoothed) values of C, the specific heat for the three samples of differing crystallinities. The extrapolation to both 0% and 100% was performed every .04° and the results were fitted to equation 3.2, the same as the real samples.

Appendix D presents the extrapolated data, and figure 2 is a

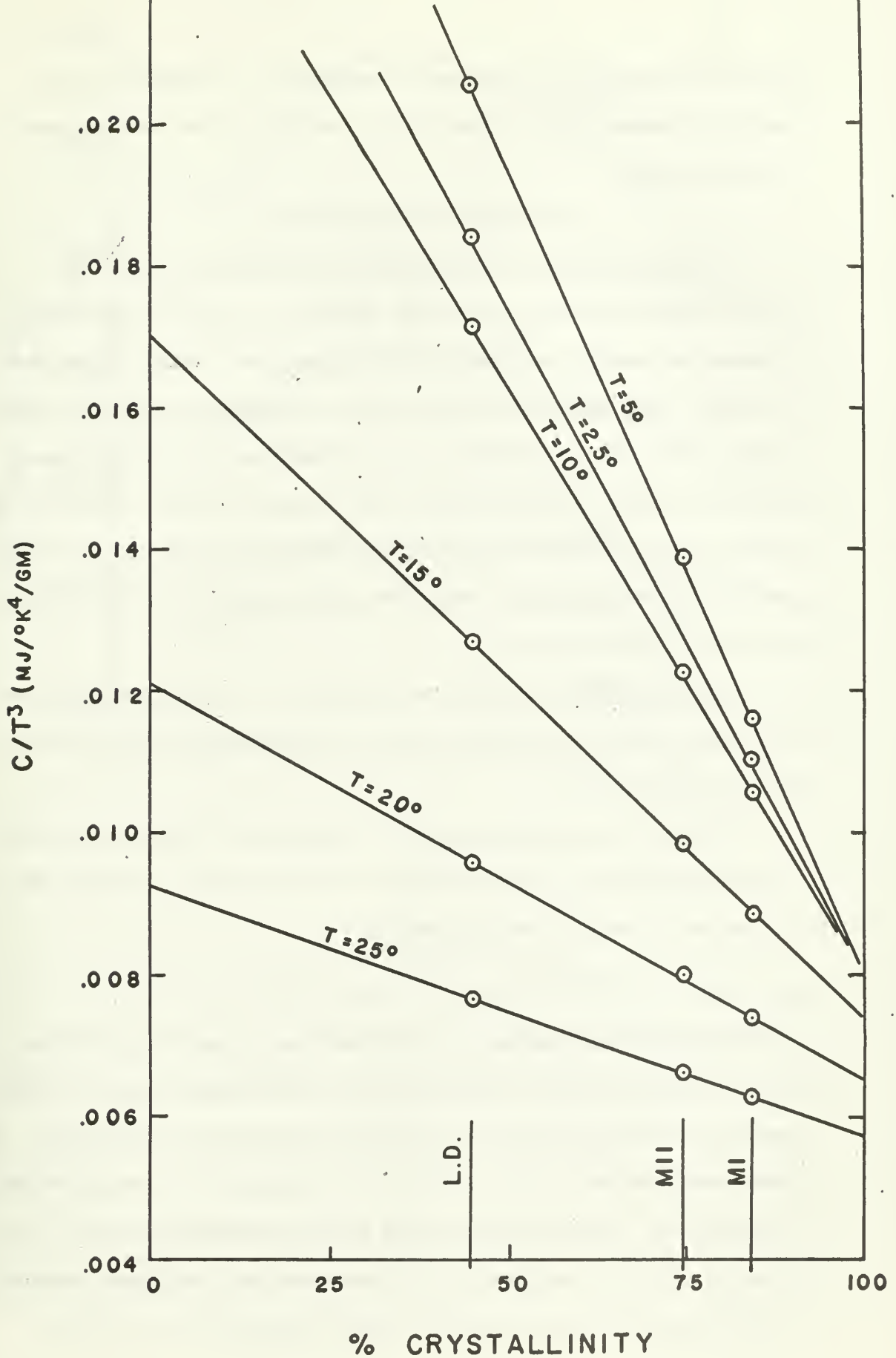

Figure 3. C/T^3 versus crystallinity.

plot of the specific heat versus temperature. In Appendix E are shown the parameters for equation 3.2 for all of the real and extrapolated samples.

The 100% Extrapolated Data

The heat capacity obtained from the extrapolation to 100% crystallinity had some interesting features. A plot of C/T^3 versus temperature shows a relatively large temperature region (up to about 9^oK) where the specific heat has a cubic temperature dependence (figure 4). This is in agreement with the expectations if there exist relatively large binding forces in the crystalline case, since on the basis of the Debye model larger forces imply larger θ's which in turn imply an increase in the temperature range in which the cubic dependence holds (equation 1.7).

For this case, an excess heat capacity is not indicated by the C/T^3 plot, nor is one expected since this material should be a continuous polycrystal.

When the heat capacity for this hypothetical sample is plotted against temperature on log-log paper, it is possible to obtain the parameters A and a of the expression,

$$C = AT^a. \qquad 3.5$$

There appeared two regions in which they were constant, indicating that the specific heat is proportional to some power, a, of the temperature. The first region was the cubic dependence noted before. The other was from about 20 to 26^oK where the exponent, a, was approximately 2.37-2.40. In between the value decreased uniformly. This is in disagreement with the prediction of Genensky and Newell who expected it to be equal to some constant slightly greater than 2.5 for an

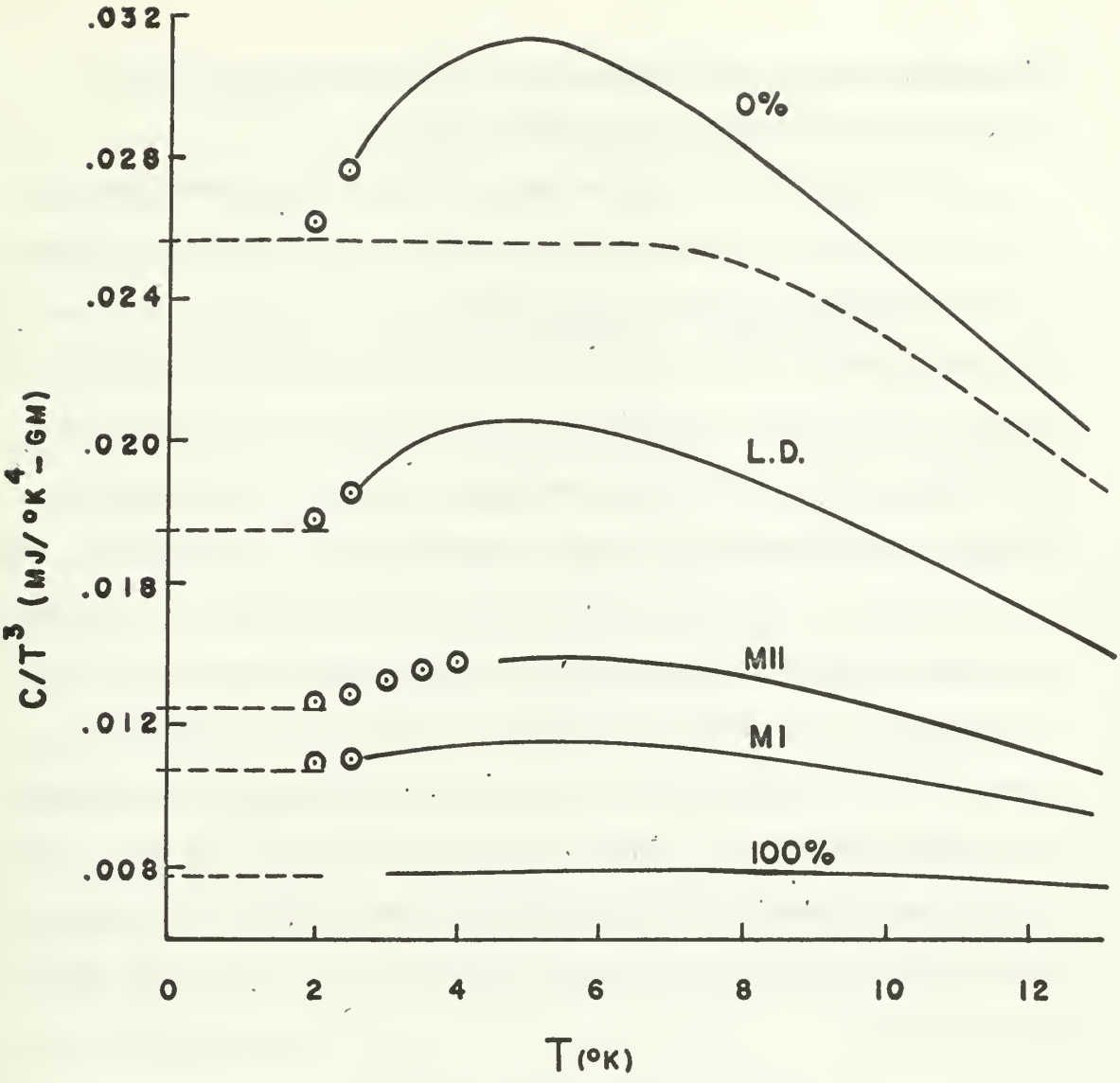

Figure 4.

A plot of C/T^3 versus temperature for polyethylene, where the solid lines are the experimental and the extrapolated data, the dotted line below the 0% curve is the data minus the Einstein term, and the other dotted lines are the predicted $T = 0^{\circ}K$ values for these samples. The dots represent the predicted specific heat values in all cases.

appreciable temperature region, for a crystalline polymer [19]. This contradiction will be discussed later.

The Tarasov model could be well fitted to the extrapolated data. The method used to determine the parameters was essentially the same as that suggested by Wunderlich, except that the equations used are for the extended model, equation 1.19 rather than the one suggested by Tarasov, which doesn't separate the longitudinal and transverse contributions [52]. According to equation 1.22 there should exist a region in which the heat capacity becomes linear in temperature. This will occur at a temperature well above that at which most of the three dimensional modes are filled and above the temperature range of this investigation. Therefore the data of Dainton, et al, giving the specific heat of polyethylene from 20-300°K, were used to determine the linear region [13]. This procedure will be justified later. The linear region appears to occur between 80 and 110°K, where C/T has the value 6.69mj/°K^2-gm. Rewriting equation 1.22, it is seen that in this region,

$$C/T = \pi^2 R \left[\frac{1}{3}\left(\frac{2}{\theta_{1T}} + \frac{1}{\theta_{1L}}\right)\right]. \qquad 3.6$$

Another relation between θ_{1T} and θ_{1L} is necessary to determine them uniquely. This was accomplished by considering that the θ_{1L}, since it was the longitudinal mode limit for the chain, might be well characterized by the largest frequency for which the C-C bond will be stretched. Reference to the Raman spectrum of polyethylene indicates a value of 1150 cm^{-1} for this parameter, and therefore a value of 1655°K was assumed for θ_{1L} [15]. This fixed θ_{1T} at 707°K. (The use of an apparent optical mode in this discussion, which up to now had only considered acoustical vibrations, will be discussed later).

Having determined these two parameters, it is then necessary to fix the remaining two thetas needed for the extended Tarasov model, Θ_{3T} and Θ_{3L}. One relation comes from equation 1.20, which is here rewritten,

$$3.7 \qquad C/T^3 = 3R\,\frac{4\pi^4}{5}\left[\frac{1}{3}\left(\frac{2}{\Theta_{1T}\Theta_{3T}^2} + \frac{1}{\Theta_{1L}\Theta_{3L}^2}\right)\right].$$

This is the low temperature limit, where C/T^3 is constant, and the results below $\sim 9^{\circ}K$ could be used to evaluate the left hand side. In order to solve for either Θ_{3T} or Θ_{3L} another relation is needed. This was obtained from sound velocity measurements at liquid nitrogen temperatures for a highly crystalline sample. These measurements were performed by Professor W. Reese [33]. Extrapolation of the results to zero degrees Kelvin predicted that the ratio of the longitudinal sound velocity to that of the transverse was 1.67. Since the thetas have the same relative relationship to one another as do the sound velocities, Θ_{3T} and Θ_{3L} could now be determined. The Tarasov parameters for this case are found in Table III.

The 0% Extrapolated Data

Extrapolation to the 0% crystallinity (completely amorphous) case led to results which were quite different from those discussed above. In particular, the plot of C/T^3 versus the temperature shows that the heat capacity was not proportional to the cube of the temperature anywhere. The curve starts with a positive slope at $2.5^{\circ}K$, increases to a maximum at around $5^{\circ}K$, then decreases uniformly. This is also the case for the real samples as can be seen in figure 4. Since even the Marlex I sample (crystallinity of 84.1%) displays this hump, while the 100% extrapolated sample does not, it is quite apparent

that the presence of the hump must be due to the amorphous polyethylene. The hump is interpeted as an indication of an excess heat capacity. Referring to the first section the heat capacity for the lowest temperatures should then be of the form,

$$C = AT^3 + \gamma E\left(\frac{\theta_E}{T}\right) \tag{3.8}$$

$$\gamma = 3k_B N_E \tag{3.9}$$

where γ, A and θ_E are constants to be determined. This equation was best fitted, in the least squared sense, to the extrapolated results (and to the Low Density data where a correction was applied to account for the crystalline part) to yield values for γ, A and θ_E. For the model which describes the portion of the heat capacity not given by the Einstein term, one is forced to accept a continuum type, since it is not possible to do lattice dynamics for the amorphous case. From the foregoing discussion, the extended Tarasov model was chosen. Assuming this, A is interpeted as

$$A = \frac{4\pi^4}{5}(3R - \gamma)\left[\frac{1}{3}\left(\frac{2}{\theta_{1T}\,\theta_{3T}^{\frac{1}{2}}} + \frac{1}{\theta_{1L}\,\theta_{3L}^{\frac{1}{2}}}\right)\right]. \tag{3.10}$$

There is no reason to assume that the one dimension parameters will change from those used previously, since they are merely functions of the forces along the chain. However another relation between θ_{3T} and θ_{3L} is still needed in order to determine them uniquely. The ratio of the longitudinal and transverse sound velocities used earlier is not really applicable in this case, since the sound velocities were those for a highly crystalline sample; but, lacking any other evidence, the same relation was assumed.

Using the above assumptions, and the values of A and γ, the

Tarasov parameters can be found. They are presented in Table III along with other results for this extrapolated hypothetical sample.

Summary

The percentage difference between the 0% and the 100% extrapolated samples were plotted against temperature as shown in figure 5. Although the curve is approaching zero, it is impossible to determine with any degree of certainty when if ever this would occur. However, it is felt that the percentage difference would be insignificant by 100°K, where the data is linear in temperature [13]. This supports the assumption that Θ_1 will be the same for all samples.

The heat capacities for the real samples and the extrapolated ones are shown in Appendix D at .5°K increments, together with the specific heats predicted by the Tarasov equation, equation 1.19, which is here expanded as

3.11
$$C = R\left\{X\left[2\left\{D_1\left(\frac{\Theta_{1T}^{100}}{T}\right) - \frac{\Theta_{3T}^{100}}{\Theta_{1T}^{100}}\left[D_1\left(\frac{\Theta_{3T}^{100}}{T}\right) - D_3\left(\frac{\Theta_{3T}^{100}}{T}\right)\right]\right\}\right.\right.$$
$$\left.\left. + \left\{D_1\left(\frac{\Theta_{1L}^{100}}{T}\right) - \frac{\Theta_{3L}^{100}}{\Theta_{1L}^{100}}\left[D_1\left(\frac{\Theta_{3L}^{100}}{T}\right) - D_3\left(\frac{\Theta_{3L}^{100}}{T}\right)\right]\right\}\right]$$
$$+(1-X)\left(1 - \frac{\gamma}{3R}\right)\left[2\left\{D_1\left(\frac{\Theta_{1T}^{0}}{T}\right) - \frac{\Theta_{3T}^{0}}{\Theta_{1T}^{0}}\left[D_1\left(\frac{\Theta_{3T}^{0}}{T}\right) - D_3\left(\frac{\Theta_{3T}^{0}}{T}\right)\right]\right\}\right.$$
$$\left. + \left\{D_1\left(\frac{\Theta_{1L}^{0}}{T}\right) - \frac{\Theta_{3L}^{0}}{\Theta_{1L}^{0}}\left[D_1\left(\frac{\Theta_{3L}^{0}}{T}\right) - D_3\left(\frac{\Theta_{3L}^{0}}{T}\right)\right]\right\}\right]\right\}$$
$$+(1-X)\,\gamma E\left(\frac{\Theta_E}{T}\right).$$

The superscripts on the Θ's refer to either the 0% or the 100% parameters, which are presented in Table III. The crystallinities, X ,

are shown in Table I.

Two hitherto undefined terms also appear in Table III. These are the Tarasov parameters which would result if no separation into the longitudinal and transverse modes were assumed, which is the original model discussed by Tarasov. In this case, equation 3.11 would become,

$$3.12 \qquad C = 3R\left\{X\left[D_1\left(\frac{\theta_1^{100}}{T}\right) - \frac{\theta_3^{100}}{\theta_1^{100}}\left[D_1\left(\frac{\theta_3^{100}}{T}\right) - D_3\left(\frac{\theta_3^{100}}{T}\right)\right]\right]\right.$$

$$\left. + (1-X)\left(1-\frac{\gamma}{3R}\right)\left[D_1\left(\frac{\theta_1^{0}}{T}\right) - \frac{\theta_3^{0}}{\theta_1^{0}}\left[D_1\left(\frac{\theta_3^{0}}{T}\right) - D_3\left(\frac{\theta_3^{0}}{T}\right)\right]\right]\right\}$$

$$+ (1-X)\,\gamma E\left(\frac{\theta_E}{T}\right).$$

In addition, the classic Debye temperature is shown as calculated from the low temperature limit.

In figure 4 the dotted line beneath the 0% crystallinity sample curve is the result of subtracting the term $\gamma E\left(\frac{\theta_E}{T}\right)$ from the data, to illustrate how it accounts for the excess heat capacity. For the other samples, the dotted lines indicate the $0^{\circ}K$ intercept, and for all cases, the circled points are the values predicted from equation 3.11.

In Appendix D the smoothed values of the specific heat for each sample is shown, along with the calculated specific heat of the Tarasov model as given by equation 3.11. This calculation was performed by the computer (the mass of the polyethylene vibrating unit is taken as 14.1 atomic mass units).

Table III

The Debye, Tarasov, and excess heat capacity parameters, and the low temperature values of the specific heat for the extrapolated data.

		100%	0%
γ	(mj/°K-gm)	0.0	3.24
Θ_D	(°K)	260.1	175.4
Θ_1	(°K)	873.9	873.9
Θ_3	(°K)	141.9	78.6
Θ_{1L}	(°K)	1655.0	1655.0
Θ_{1T}	(°K)	707.0	707.0
Θ_{3L}	(°K)	222.8	123.4
Θ_{3T}	(°K)	133.7	74.1
Θ_ϵ	(°K)	-	23.0
$\frac{C-\gamma\epsilon(\frac{T}{\Theta})}{T^3}$	(mj/°K^4-gm, low temp.)	.00787	.0256

Accuracy of the Results

To estimate the accuracy of the heat capacity data, four sources of error were considered; the determination of the amount of heat introduced into the sample, the temperature determination, the effect of the shield, and the heat capacity of the addenda.

The amount of heat energy introduced into the sample was obtained from three measurements; voltage, current, and time. The voltages (and current) could be determined to six places on the potentiometer. Since the same power was used on from four to six successive measurements, it was possible to check the reproducibility of the readings. Only at the very highest temperatures, where the resistance of the heater was probably changing with temperature, did it vary as much as .1%. The current measurement had the same inconsistency, but since it was

determined by measuring the voltage across a standard resistor, it also had an inherent maximum error of .05%. Timing was presumed accurate to one part in thirty thousand. The maximum total error from this source is therefore estimated to be .05% at the low end of the temperature scale and .25% at the high end.

As discussed in Appendix A, the thermometers were assumed correct to within .5% of the absolute temperature. This uncertainty will influence the accuracy of the heat capacity results in two ways. Since a temperature difference is divided into the total heat to obtain the heat capacity, an error can arise there. However any experimental or systematic errors in the temperature determination will be the same over a short temperature interval and should cancel out (this is ensured by the use of the smooth fitted curve which should average out these errors). Therefore the possible error from this source should be only that due to the error of judgment in reading the resistance bridge. This results in uncertainties in the heat capacity determination of .12% at 2.4°K up to about .2% at 30°K.

The other manner in which the inaccuracy of the temperature scale enters into the error is in assigning a temperature to a particular heat capacity measurement. Since the specific heat can be expressed at any point as being proportional to some power of the temperature (the exponent will be between 3 and 2.4 for this case), the percentage error in the specific heat will be larger than that of the temperature. In this case the maximum possible error amounts to 1.5% at the lowest temperature and 1.2% at the highest from this source.

Since it was impossible to completely isolate the sample from

the shield thermally, considerable care had to be taken to ensure that they were at the same temperature, to prevent possible heat leakage. Experimentally, the effects of large temperature differences were investigated, by purposely overshooting the shield temperature and observing the effect it had on heat capacity data. On the basis of these experiments it was decided that, with the experimental procedures used when actual data were being taken, this contribution to the error could be neglected for all but the highest temperatures, when, due to the insensitivity of the shield thermometer, difficulty insuring equal temperature of the shield and sample might occur. At these temperatures, the error might approach .5%.

The heat capacity of the addenda was measured over the entire temperature range, so that it could be applied as a correction to the total measured for any sample. Since the mass of the addenda was chosen to be as small as possible, so that its heat capacity would be on the order of 10% of that of the samples, any possible errors which are present in the measurement of its heat capacity would be reduced by a factor of ten when applied to the total possible error for a sample. Considering the preceeding this uncertainty amounts to approximately .2% over the entire temperature range.

Considering all of the above, it is felt that the measured heat capacities were accurate to within 1.9% for the temperature up to about 26^{o}K, and 3% above that.

The subject of Appendix B is the measurement of the specific heat of copper. The results are compared with data found in the literature which presumably is of higher precision and accuracy than this work. The comparison shows that the results are consistant,

within the error estimate, but the present results tend to be low over most of the temperature range, which could be an indication of a systematic error. This point was not investigated further.

As mentioned before, there was no statistical criteria established for rejecting any of the data, and the only points discarded were ones in which a large deviation could be attributed to a blunder in data accrual.

When the data were fitted to equation 3.2, the RMS deviation (Table II) was found to be well within the estimated accuracy of the experiment and therefore the use of the smoothed data is considered to be a valid representation of the results.

Since one of the objectives of this investigation was to verify the density (crystallinity) dependence of the specific heat of polyethylene, and an extrapolation was made to the hypothetical 100% and 0% crystalline phases, an estimate was made as to the reliability of this. The heat capacity of the three real samples would be exactly linear in crystallinity over the entire temperature range, if a variation of at most 4% were made in any one of the heat capacities, or if a 1.5% adjustment were made in one of the crystallinities. Additionally there are other combinations of adjustments which could be made, but it is the uncertainty in the degree of crystallinity which is believed to be subject to the most error. As noted in Table I, there is an inherent, approximate 2% error which is due solely to the uncertainties in the densities. In addition, since the densities of the amorphous and crystalline phases are not well established, it is estimated that the crystallinity of a sample could be in error as much as 4%, based on the density method of determining crystallinities

(equation 1.1). In view of this, it is felt that the linearity is valid to the precision of this experiment.

Due to the possible error in the crystallinities, the accuracy of the extrapolated samples can be better than 2% for the amorphous case, and .8% for the crystalline phase. The uncertainties which are present in the actual specific heat is taken over into the extrapolated data. If the relative error in the heat capacity at any particular temperature is the same for all of the samples, as should be expected since they should exhibit the same systematic error if it is present, the maximum possible error in the extrapolated data due to this cause will be the same, or about 1.9% over most of the temperature range. Thus the uncertainty in these figures will be approximately 3 and 4% for the completely crystalline and amorphous phases.

The precision of this experiment can be estimated by the closeness of the fit of the actual data points to the smoothed curve given by equation 3.2. The deviations appear random and the per cent RMS deviation is given in Table II, where the % RMS deviation is defined by,

$$3.13 \qquad \%\text{RMS} = 100\% \left(\frac{\sum_{i=1}^{N} \left(\frac{C_i - C}{C_i} \right)^2}{N} \right)^{1/2} .$$

This precision, which is also an estimate of the reproducibility of the results, is between 1.01 and 1.52% for the polyethylene samples.

4. CONCLUSIONS

Comparison with Other Results

The results of this research have been compared with all of the known experimental work on the specific heat measurements on poly-

ethylene in their common temperature ranges. A detailed survey of these comparisons follows:

(a) Isaacs and Garland [21]

The specific heat measurements of Isaacs and Garland were on a single high density sample in the temperature range 1.8 to 5.3°K. They assumed that the specific heat in this range displayed T^3 dependence and therefore did not separately determine the heat capacity of the addenda, but rather calculated it and subtracted it from the total. This led as they report to an unaccountable deivation from the T^3 behavior, but they attributed it to experimental error. However it is felt that they were in reality observing the excess heat capacity which was disguised by their method of analysis.

For the comparison in the mutual temperature range, it was noted that both the amorphous and crystalline parts of polyethylene are proportional to the cube of the temperature if the Einstein term is subtracted. Since their sample did not have the same degree of crystallinity of any of the ones measured in this work, the following equation was used to determine what specific heat should be expected on the basis of the present results;

$$C = X(.00787)T^3 + (1-X)\left[.0256\,T^3 + 3.24\,E\left(\frac{23^{\circ}K}{T}\right)\right] . \qquad 4.1$$

This is merely the low temperature limit of equation 3.12 with the measured values inserted. This assumed no model, however; only that the specific heat be T^3 dependent at low temperatures, which it is for any realistic case, and that the linearity in crystallinity is valid. For the crystallinity of Isaacs and Garland's sample, two values were investigated; first the reported X-ray determined result

of 90%, and second, a crystallinity of 85% deduced from the reported density. In Table IV where the comparison is made, the two different values for the C/T^3 resulting from the different crystallinities are subscripted to distinquish them.

Examination of the table shows that the value deduced from this work with the density determined crystallinity is in excellent agreement with Isaacs and Garland's, if it is recognized that they could not separate the excess heat capacity. Use of this crystallinity rather than the X-ray value contains a certain amount of consistency since the present results were based on the density measurements. It is noted they give no estimate of the possible error in the X-ray value, although it is doubted that it is as high as 6%.

Table IV

Comparison of present results with those of Isaacs and Garland. (Values expressed in $mj/^oK^4$-gm)

	$C/T^3_{(I\&G)}$	$C/T^3_{(90\%)}$	$C/T^3_{(85\%)}$
$T = 2^oK$	.0113	.0097	.0108
3	.0113	.0100	.0112
4	.0113	.0102	.0115
5	.0113	.0103	.0116

(b) Reese and Tucker [34]

The results of thermal conductivity measurements on three samples of polyethylene were used by Reese and Tucker to indirectly determine the specific heats of the samples. This led to a low precision averaged set of values over the temperature range 1 to 4.5^oK. The comparison with the present work was made in the same manner at it was for Isaacs and Garland's work, and equation 4.1 was again used.

However in order to compare the values, a conversion was necessary. All of the results of Reese and Tucker were in terms of volume percentages of crystallinities and the specific heats were in units of $mj/^oK^4\text{-}cm^3$. The values used below are not as reported, but have been converted using their values of the densities.

The present investigation was not independent of the work of Reese and Tucker, and, in fact, was an outgrowth of it. Therefore the same types of polyethylene were used in both experiments. However slightly different densities (crystallinities) were found for the samples of the two investigations. This is explained by the different molding processes, and cooling times, which is known to effect the degree of crystallinity [31].

The comparison is shown in Table V. The sample names are from the work of Reese and Tucker and should not be confused with the same names used in the present work. The calculated crystallinities are shown in the table.

These results are in agreement within the reported error given by Reese and Tucker (10%) except for Marlex I. However in view of the indirect methods of their measurements, it is not considered excessive. In addition they report a "dish shape" characteristic if the values of C/T^3 is plotted against temperature. This was proposed to be due to a lack of precision in the temperature and thermal conductance determinations at the two temperature extremes of their range. If it is assumed that this was the case at only the low end, then the points above 2^oK will display one half of the "dish" and will appear as the curves in figure 3 between 2 and 4.5^oK. This is believed to have been the case since at the lowest temperatures, the parameter from

which the heat capacities was deduced (the thermal equilibrium times) would be greatly increased due to the thermal resistance at the sample-low temperature sink interface. In light of the above, the results are considered to be in good agreement.

Table V

Comparison of present results with those of Reese and Tucker (Values expressed in $mj/^{o}K^{4}$-gm)

T (^{o}K)	$C/T^{3}_{(R\&T)}$	$C/T^{3}_{(Present)}$
	Marlex I (X = 79%)	
2	.0147	.0118
3	.0147	.0124
4	.0147	.0128
5	.0147	.0129
	Marlex II (X = 62%)	
2	.0166	.0149
3	.0166	.0159
4	.0166	.0167
5	.0166	.0168
	Low Density (X = 47%)	
2	.0210	.0175
3	.0210	.0190
4	.0210	.0200
5	.0210	.0202

(c) Sochava [44]

As mentioned in the introduction, the specific heat measurements reported by Sochava for the temperature range 17 to $60^{o}K$ are on a sample of unknown density. Since it has been shown here that the

specific heat below 30°K is strongly density dependent, comparison is difficult. However, if Sochava's data are placed on a specific heat-crystallinity plot from the present work and are adjusted to fall on the straight lines, a crystallinity of 53% is determined for Sochava's sample. This is a reasonable value for commercial polyethylene, and it is felt that, as far as the comparison can be made, there is agreement between the two sets of data.

(d) Dainton, Evans, Hoare, and Melia [13]

Dainton, et al, reported measurements on the specific heat of two samples of polyethylene for the temperature range 20 to 300°K. Their two samples were of very similar crystallinity (78 and 79%), and due to the manner in which the data were presented, comparison could be made only at 20 and 30°K. Again the crystallinity was deduced from the reported density (it was given for only one sample), but in this case it was identical with that given as determined by X-ray methods. To make the comparison predictions from the present results had to be adjusted to 78 or 79% crystallinities. This was accomplished by plotting the specific heat versus crystallinity for the three measured samples at 20 and 30°K, connecting the points with a straight line, and finding the specific heats corresponding to the reported crystallinities. Table VI shows the results of this prediction, along with the results of Dainton's et al. The subscripts 78% and 79% refer to the two samples.

Table VI

Comparison of present results with those of Dainton, et al. (Values given in mj/°K-gm)

	Dainton, et al		Present work	
	$C_{78\%}$	$C_{79\%}$	$C_{78\%}$	$C_{79\%}$
T = 20°K	66.8	62.1	62.2	61.6
30	147.0	146.2	146.7	146.4

Considering that the 20°K results reported by Dainton, et al, are extrapolated from 22°K (the lowest temperature of actual measurements), the agreement is felt to be excellent.

The Tarasov Model [47]

The present results show clearly that a strong specific heat-crystallinity dependence is evident in polyethylene below 30°K. Hence no single set of Tarasov parameters can be expected to predict the heat capacity in general, and therefore a choice was made to separate the contributions of the two phases, amorphous and crystalline, and obtain two sets of thetas. But they are not completely independent, as will be discussed.

The density dependence does not extend much beyond the temperature range of this investigation. This was determined from the fact that the results of Sochava and Dainton, et al, are essentially the same above 50°K, whereas they had differed by over 10% at 30°K. Additionally data from Dainton, et al, on a sample of crystallinity 58% above 90°K show that the specific heat for this sample is the same as for the more crystalline ones. (Above 110°K this is no longer true, but it is due to effects which are of no concern here). This compares well with the indications of figure 5 which is a plot of the relative difference between the amorphous and crystalline results

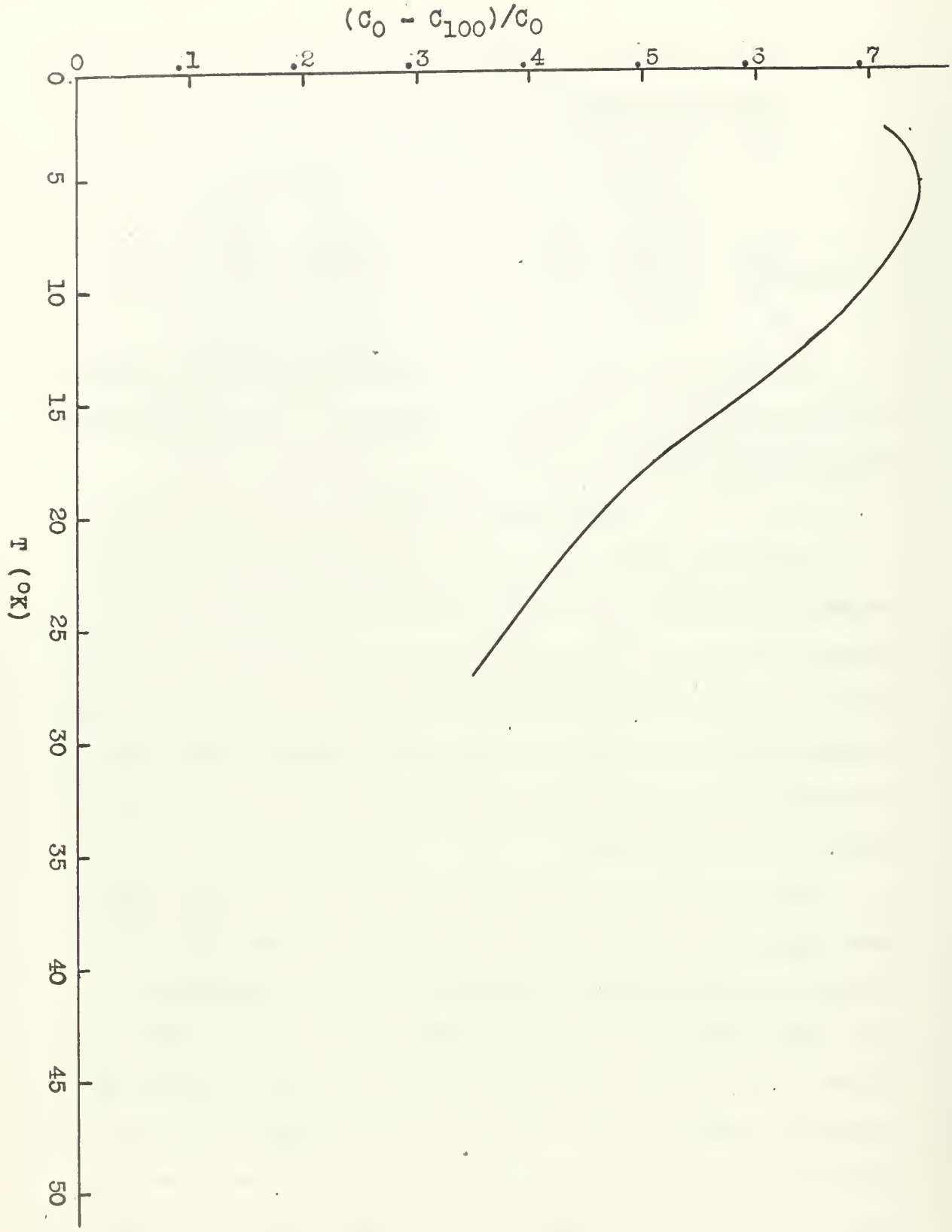

Figure 5. Relative difference between the 0% and 100% extrapolated data versus temperature.

below 30°K. From the figure it is clear that the difference will be quite small for temperatures above about 60°K, if the curve is extrapolated above 30°K.

The disappearance of the density dependence at the higher temperatures has a rather natural explanation also on the basis of the Tarasov model. The three dimensional parameters associated with the two phases are small, which implies that the three dimensional modes will be nearly all filled at not very high temperatures. Thus the major contribution to the specific heat should be due to the one dimensional vibrations, which are assumed the same for both phases.

The assumption that the one dimensional parameters are the same in both the amorphous and crystalline cases is based on the fact that these parameters are associated only with the forces along the chains which should be independent of the configuration the chain has assumed. It is also within the temperature range in which the density dependence disappears that the specific heat becomes linear in temperature, as is predicted by the Tarasov model, and it was from this temperature region that the one dimensional thetas were determined. The linear portion of the specific heat-temperature curve yielded only an average value of the thetas, and more information was needed to separate it into the longitudinal and transverse parts.

The assumed value of 1655°K for the longitudinal one dimensional theta was based on the measured maximum frequency associated with the C-C stretch of the polyethylene chain as determined by Raman spectrum [15]. Since this parameter had been taken to be related to the maximum acoustic frequency along the chain, the use of what appears to be an optical mode may not be valid, but this seemed physically

representative of what this mode should be. In any event it should be pointed out that the predicted specific heat on the extended Tarasov model is relatively insensitive to variations of the values of θ_{1T} and θ_{1L} as long as the relation

$$4.2 \qquad \frac{1}{\theta_1} = \frac{1}{3}\left(\frac{2}{\theta_{1T}} + \frac{1}{\theta_{1L}}\right)$$

is satisfied. For example, if the ratio of θ_{1T} to θ_{1L} is taken to be .6 (the same ratio as assumed for the three dimensional case), it changes the specific heat preduction at 20°K by only .5%.

One further remark must be made on the one dimensional parameters. On the basis of experimental data, obtained by neutron diffraction, the upper limit of the bond stretching acoustic mode observed in polyethylene was found to be 545 ± 25 cm^{-1} [32]. This corresponds to a characteristic temperature of 785 ± 35°K. If this value is assumed for the θ_1, it predicts specific heats which are much too high from about 12°K on up in temperature. This is interpeted not as anything wrong with the value of the maximum frequency noted above, but rather an indication that there is no real physical significance of the characteristic temperature from the continuum model.

The three dimensional thetas for the amorphous and crystalline parts differ from one another in the manner in which they should be expected. They are related to the forces acting between the polyethylene chains, and, since the forces are most probably of the type which decrease rapidly with distance, the less dense and less closely packed chains of the amorphous state should have smaller thetas. The three dimensional parameter deduced from the experimental data support

this qualitative description.

The calculated values of the specific heat based on the original Tarasov model are not in good agreement with the experimental results. As can be seen in Appendix D, there is a 5-6% difference around 20°K, although in other temperature ranges the fit is better. The extended Tarasov model, which separated the longitudinal and transverse contributions, was used since it gave an approximately 2-4% improvement over the entire range when compared with the basic model. However in the final analysis the Tarasov model should not be expected to explain the specific heat of polyethylene any more than the Debye theory can for other solids, since they contain inherent erroneous assumptions concerning the lack of dispersion. In view of this, the fact that the Tarasov model fits as well as it does makes it useful as a first approximation for the specific heats of fibrous solids such as polyethylene at low temperatures.

The Stockmayer-Hecht Model [19,46]

In order to investigate the applicability of the model of Stockmayer and Hecht as expanded by Genensky and Newell, the specific heat of the 100% crystallinity case was the only one considered, as the model was suggested for a fibrous crystalline solid. At the lowest temperatures, the model did predict the cubic temperature dependence, but the predicted temperature region for which the specific heat would be proportional to $T^{2.5+}$ was not found. However it is felt that this was an over simplification on the part of Genensky and Newell for, even if their analysis were correct, it would not be rigorously reflected by this relation. The reason for this is that they predict in some temperature region the specific heat should be

4.3 $$C = AT^{5/2} + BT^3$$

where A and B are constants (the first term is the contribution of the interchain interactions and the second is the result of vibrations along the chains). This prediction does not give any appreciable temperature region in which the specific heat is proportional to a constant power of the temperature.

To test the model for the temperatures at which the specific heat was investigated, a plot of $C/T^{5/2}$ versus the square root of the temperature should have a region where the slope is constant, if the model is correct. Figure 6 shows that this does not occur in the temperature range below $30^{o}K$, and, since the slope is negative at the high temperature end, it is doubted that it will occur.

However, as is also shown in figure 6, plotting C/T versus $T^{3/2}$ does show a linear region (22 to $27^{o}K$) which implys

4.4 $$C = AT^{5/2} + BT .$$

This could be interpeted as implying that their analysis is incorrect in the sense that they do not anticipate that the linear temperature contribution from the vibrations along the chain would occur at the same temperatures that the $T^{5/2}$ relation holds for the interchain specific heat part. However, this cannot be reconciled with the model as presented, because the relative size of the two contributions is wrong.

It is not possible in practice to draw from experimental heat capacity data reliable inferences regarding the detailed form of the frequency distribution, as the heat capacity tends to smooth out the individual features of the frequency distribution. Hence the compar-

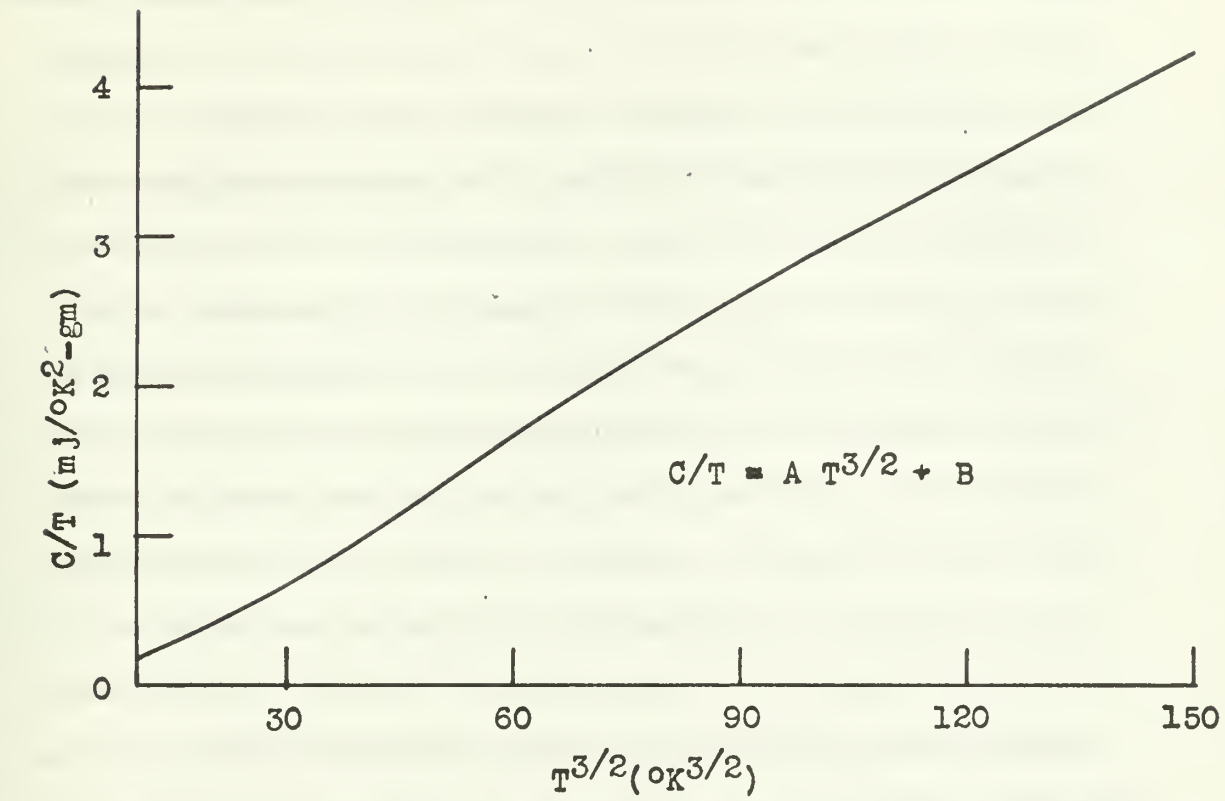

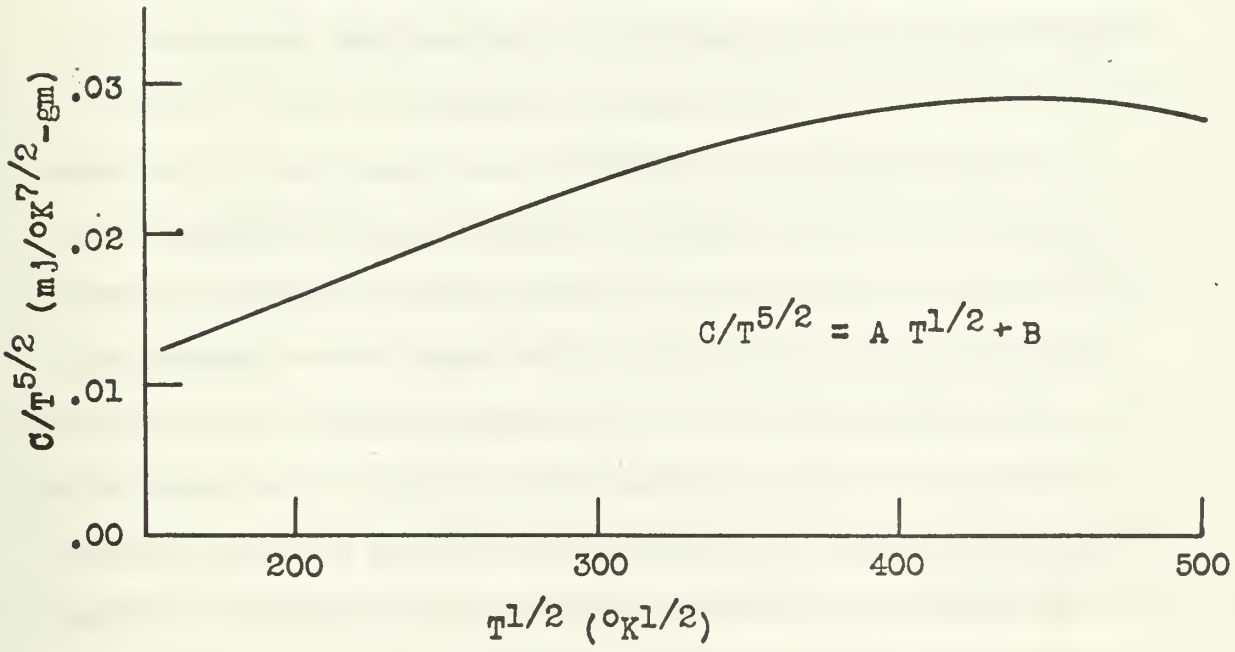

Figure 6. C as two functions of the temperature.

ison with the model of Stockmayer and Hecht cannot specifically determine where their analysis is in error. On the basis of the apparent $T^{5/2}$ relation for the interchain specific heat contribution (if the interpetation of figure 6 is correct), it seems that the essence of the model is correct, but that a reexamination of the one dimensional part is in order. However other assumptions of theirs may be wrong. Since the polyethylene crystal appears to be lamellae, (although not directly observed in the bulk polyethylene) and the crystalline form is spherulitic, the structure may be such that the idealized tetragonal crystal, assumed by Stockmayer and Hecht, will not yield the correct predictions. Moreover since they had to make estimates of the relative sizes of the force constants, of which little is known, erroneous assumptions here could lead to different forms for the frequency spectrum, and thereby errors in the deduced heat capacity. In any event in its present form the specific heat predicted from this model is not completely applicable to polyethylene below 30°K.

The Excess Heat Capacity

In the absence of any acoustical measurements made at low temperatures for the heat capacity of polyethylene, the humping of the C/T^3 versus temperature curve, figure 4, was interpeted as an excess heat capacity. The appearance of this excess was not expected, but it is not unreasonable that it does appear when it is recognized that it is present in other amorphous solids [4,12,17]. The origin of the excess heat capacity is unknown, but attributing it to the existence of non-acoustical low frequency modes seems reasonable. In particular, the Rosenstock theory is appealing since it is known that free volume (holes) does exist in amorphous polyethylene [10,11]. However

no reasonable conclusions can be reached on this or any other model which might explain the excess on the basis of the present results.

The addition of the Einstein term to the amorphous heat capacity empirically fits the data quite well at the low temperatures, and no other correction is deemed necessary to account for the excess in an analytic expression for the specific heat. In fact, it is felt that when low temperature acoustic measurements of the specific heat of polyethylene become available, the value for the extrapolated $T = 0^{o}K$ point will agree with the following relation which is based on the present results;

$$C = (.0256 - .0178X)T^{3}. \qquad 4.5$$

From the size of the constant which multiplies the Einstein function, it is readily deduced that of all of the possible vibration modes of the solid, only .17% are taken up in the excess term. This can be compared with the number of these modes in vitreous germanium (.4%) and vitreous silica (2%), but no conclusions can be drawn [4,17].

Summary

As has been shown, both the continuum, Tarasov, model and the lattice dynamical, Stockmayer-Hecht, model fail to completely predict the specific heat of polyethylene. This is not surprising as they are based on models which cannot be exact for differing reasons. The continuum model is at best a first approximation since it ignores the dispersion of the sound velocity which surely takes place in any real solid. Hence the spectrum of vibrational states is wrong. But, considered as a simple two parameter approximation, the predictions are very good. The Stockmayer-Hecht model which attempts to account for

the dispersion fails for different reasons. Since this model is based on an assumption of the interparticle forces in various directions, there are many parameters which determine the predictions. If some are chosen incorrectly, the whole model fails. On the basis of the present results no attempt was made to evaluate the parameters, since one of the basic predictions of the model did not materialize.

The Einstein term adjustment for the excess heat capacity found in the amorphous polyethylene was adequate to explain the departure from the cubic temperature dependence of the specific heat at the lowest temperatures. But until such time that empirical evidence is brought forward to verify some model to explain it completely, it must remain as an a posteriori addition to explain the experimental results.

The hypothesis that the specific heat of polyethylene is linear in crystallinity was proven, it is felt, in the temperature range covered by this investigation, and extrapolation to the completely amorphous and completely crystalline cases is considered valid. It is also believed that the crystallinity dependence has disappeared by 50-60°K (considering only the temperatures below 110°K).

The present low temperature specific heat measurements are more reliable than those given by the prior investigations (Isaacs and Garland, and Reese and Tucker), since the existence of the excess heat capacity is recognized. By extrapolating these results to 0°K and by using the method of interpolating between crystallinities noted before, this work can be mated to that of Dainton, et al, to give a continuous specific heat-temperature coverage up to 110°K, where many other data become available. The resulting information

should prove valuable to workers investigating models of crystalline and non-crystalline fibrous solids into which nearly all polymers can be classed.

ACKNOWLEDGMENTS

I wish to thank Professor William Reese for his patient and enthusiastic guidance in this work, and Mister Lynwood F. May for his technical assistance in the construction of the equipment.

BIBLIOGRAPHY

1. G. Ahlers, Rev. Sci. Instr., 37,477(1966)

2. O.L. Anderson, J. Phys. Chem. Solids, 12,41(1959)

3. O.L. Anderson and G.J. Dienes, "The Anomalous Properties of Vitreous Silica", Non-Crystalline Solids, (Wiley, New York, 1958)

4. A.A. Antoniou and J.A. Morrison, J. Appl. Phys, 36,1873(1965)

5. J.A. Beattie, "Gas Thermometry", Temperature Its Measurement and Control in Science and Industry, (Reinhold, New York, 1955) Vol. 2

6. M. Blackman, Proc. Roy. Soc., A148,365,385(1935)

7. M. Blackman, Proc. Roy. Soc., A149,117,126(1935)

8. F.G. Brickwedde, H. van Bijk, M. Durieux, J.R. Clement and J.K. Logan, 1958 He^4 Scale of Temperatures, NBS Monograph 10 (1960)

9. W.M.B. Bryant, quoted by reference 34

10. F. Bueche, Physical Properties of Polymers, (Interscience, New York, 1962)

11. R. Chiang and P.J. Flory, J. Am. Chem. Soc., 83,2857(1961)

12. R.S. Craig, C.W. Massena, and R.M. Mallya, J. Appl. Phys., 36, 108(1965)

13. F.S. Dainton, D.M. Evans, F.E. Hoare, and T.P. Melia, Polymer, 3,277(1962)

14. J. deLaunay, "Theory of Specific Heats and Lattice Vibrations", Solid State Physics (Academic, New York,1956) Vol. 2

15. J.A. Faucher and F.P. Reding, "Relations Between Structure and Fundamental Properties", Crystalline Olefin Polymers, (Interscience, New York,1965)

16. P.C. Fine, Phys. Rev., 56,355(1939)

17. P. Flubacher, A.J. Leadbetter, J.A. Morrison, and B.P. Stoicheff, J. Phys. Chem. Solids, 12,53(1959)

18. S.A. Friedburg, "Semiconductors as Thermometers", Temperature its Measurement and Control in Science and Industry (Reinhold, New York, 1955) Vol. 2

19. S.M. Genensky and G.F. Newell, J. Chem. Phys, 26,486(1957)

20. H.J. Hoge and F.G. Brickwedde, J. Research Natl.Bur. Standards, 22,351(1939)

21. L.L. Isaacs and C.W. Garland, J. Phys. Chem. Solids, 23,311 (1962)

22. W.H. Keesom, Helium, (Elsevier, New York, 1942)

23. A. Keller and A. O'Connor, Polymer, 1,163(1960)

24. C. Kittel, Introduction to Solid State Physics, (Wiley, New York, 1963)

25. J.E. Junzler, T.H. Geballe, and G.W. Hull, Rev. Sci. Instr., 28,96(1957)

26. H.L. Laquer, Low Temperature Thermal Expansion of Various Materials, AECD-3706 (1952)

27. A.J. Leadbetter and J.A. Morrison, Phys. Chem. Glasses, 4,188 (1963)

28. R.B. Leighton, Revs.Modern Phys., 20,165(1948)

29. F.D. Manchester, Cand. Jour. Phys., 37,989(1959)

30. D.L. Martin, Phys. Rev., 141,576(1966)

31. R.L. Miller, "Crystalline and Spheruitic Properties", Crystalline Olefin Polymers, (Interscience, New York, 1965)

32. W. Myers, G.C. Summerfield, J.S. King, J. Chem. Phys, 44,184 (1966)

33. W. Reese, unpublished laboratory notebook

34. W. Reese and J.E. Tucker, J. Chem. Phys., 43,105(1965)

35. D.H. Reneker and P.H. Geil, J. Appl. Phys., 31,1916(1960)

36. M.J. Richardson, quoted by reference 11

37. T.R. Roberts and S.G. Sydoriak, Phys. Rev., 102,304(1956)

38. M.J. Roedel, Am. Chem. Soc., 75,6110(1953)

39. H.B. Rosenstock, J. Phys. Chem. Solids, 23,659(1962)

40. H.B. Rosenstock, Amer. J. Phys., 30,38(1962)

41. H.B. Sachse, "Measurement of Low Temperatures with Thermistors", Temperature Its Measurement and Control in Science and Industry (Reinhold, New York, 1955), Vol. 2

42. R.B. Scott, Cryogenic Engineering (D. Van Nostrand Company, New Jersey, 1959)

43. R.A. Smith, Wave Mechanics of Crystalline Solids (Chapman and Hall, London, 1963)

44. I.V. Sochava, Doklady Akad. Nauk. SSSR, 130,126(1960)

45. C.A. Sperati, W.A. Franta, and H.W. Starkweather, J. Am. Chem. Soc. 75,6127(1953)

46. W.H. Stockmayer and C.E. Hecht, J. Chem. Phys., 21,1954(1953)

47. V.V. Tarasov, J. Phys. Chem., 24,111(1950)

48. H. van Dijk, M. Durieus, J.R. Clement, and J.K. Logan, Physica, 24,129(1958)

49. E.R. Walter and F.P. Reding, J. Polymer Sci., 21,561(1956)

50. G.H. Wannier, Elements of Solid State Theory, (Cambridge, Cambridge, 1960)

51. H.W. Woolley, R.B. Scott and F.G. Brickwedde, J. Research Natl. Bur. Standards, 41,379(1948)

52. B. Wunderlich, J. Chem. Phys., 37,1203,1207(1962)

53. 19th Annual Calorimetric Conference, 13-16 Oct., 1964, Washington, D.C.

APPENDIX A- Calibration of the Thermometers

Introduction

Probably the most exacting aspect of this experiment was the determination of the absolute temperature scale. The difficulty stems from the fact that between 5 and 14°K there is no convenient temperature standard. Below 5°K the scale had been set by international convention in terms of the vapor pressure of liquid helium, and between 14 and 25°K, the vapor pressure of liquid hydrogen is a good standard [8,48,51]. Additionally the internationally accepted platinum resistance thermometers can be used above 10°K [20]. Between 5 and 14°K the temperature scale is normally established by means of a gas bulb thermometer.

In this investigation the resistance thermometers were calibrated below 4.2°K by means of a vapor bulb thermometer, and from 4.2 to 30°K by means of a gas bulb thermometer. Liquid hydrogen vapor pressure thermometery was not attempted due to its inherent dangers: the facilities were not available to obviate them. Initially it was planned that the platinum resistance scale was to be compared with the gas bulb results, but was not since another comparison became available (the specific heat of copper, Appendix B), and it soon appeared that the higher accuracy in temperature range above 10°K was not necessary for the purpose of this investigation.

The theory, construction and experimental procedures concerned with the calibration of the resistance thermometers is the subject of the remainder of this appendix, together with an estimate of the error in the temperature determination.

Theory of Constant Volume Gas Bulb Thermometry

The equation of state for an ideal gas is,

A.1 $$\frac{P_i V_i}{T_i} = \frac{P_f V_f}{T_f}$$

where i and f refer to the initial and final states of the system. If the volume is held constant and the initial conditions are known, then there exists a linear relation between the temperature of the gas and its pressure. A constant volume gas bulb thermometer could consist of a large volume, V, at the temperature to be measured, T, and a pressure sensing device at temperature, T_V, with volume v connected by a tube of small volume v'. Then equation A.1 must be modified to account for the fact that not all the gas is at the low temperature in the final condition; some is still in the gauge and connecting tube. To account for this equation A.1 is replaced by,

A.2 $$P_V\left(\frac{V}{T_V} + \frac{v}{T_V} + \frac{v'}{T_V}\right) = P\left(\frac{V}{T} + \frac{v}{T_V} + \int_{t=T}^{t=T_V} \frac{d(v'(t))}{t}\right)$$

where P_V is the pressure of the system when it is at T_V, and P is the pressure when the bulb is at temperature T. The integral expresses the fact that the temperature along the connecting tube varies from T to T_V. However, it is convenient to assign a temperature T_c such that,

A.3 $$\frac{1}{T_c} = \frac{1}{v'} \int_{t=T}^{t=T_V} \frac{d(v'(t))}{t} .$$

Solving equation A.2 for T, it is found that,

A.4 $$T = T_V P \frac{V}{P_V(V+v) - Pv + v'\left(P_V - P\frac{T_V}{T_c}\right)}$$

Consider now the case where $v' \sim 0$, that is assuming that the connecting tube's volume is quite small in comparison with that of the other components. Then equation A.4 becomes,

$$\text{A.5} \qquad T = \frac{P T_r}{P_r(1+\frac{v}{V}) - P\frac{v}{V}} \cdot$$

Then if $\frac{v}{V} \ll 1$, and if the bulb is at low temperature, most of the gas will be in bulb, and the pressure will be essentially linear in temperature.

However, in an actual experiment the gas will not be ideal, as implied in the previous arguments. The equation of state in this case can be written,

$$\text{A.6} \qquad \frac{Pv}{T} = R\left(1 + \frac{B_1'(T)}{v} + \frac{B_2'(T)}{v^2} + \cdots\right)$$

where the B_i''s are the virial coefficients, and v is the specific volume. If helium were used in the temperature range of the present experiment B_2' is of 2 or 3 orders of magnitude smaller than B_1', and the term containing B_2' can be neglected [22]. Since B_1' is also small, v can be set equal to $\frac{RT}{P}$ in the term which corrects for the second virial coefficient, so that,

$$\text{A.7} \qquad PV = mR(T + BP)$$

putting $\frac{B'}{R} = B$.

Using A.7 equation A.2 becomes,

$$\text{A.8} \qquad P_r\left(\frac{V}{T_r + B_r P_r} + \frac{v}{T_r + B_r P_r} + \frac{v'}{T_r + B_r P_r}\right) = P\left(\frac{V}{T + BP} + \frac{v}{T_r + B_r P} + \frac{v'}{T_c + B_c P}\right)$$

where the subscripts on the B's refer to the temperature at which they are evaluated.

Finally, consider the form that equation A.8 would take if the

initial conditions were varied somewhat, that is, by filling the system with the gas when the temperature of the bulb is at a third temperature T_N and therefore has volume V_N due to thermal contraction. Under these circumstances, equation A.8 will be,

A.9 $$P_N\left(\frac{V_N}{T_N+B_N P_N}+\frac{v}{T_r+B_r P_N}+\frac{v'}{T_c+B_c P_N}\right)=$$

$$P\left(\frac{V}{T+BP}+\frac{v}{T_r+B_r P}+\frac{v'}{T_c'+B_c' P}\right)$$

where the P_N refers to the pressure in the system when the bulb is at temperature T_N. (Notice that the T_c's on the two sides of the equation are not the same since the lower temperature is different.)

Construction Gas Bulb Thermometer

As indicated in the comment following equation A.5, temperature-pressure linearity can be obtained if the gauge volume to bulb volume ratio is made small. As a design criteria $\frac{v}{V}$ was taken as 1/20, and the connecting tube's volume v' would be held small compared to the volume of the gauge.

To obtain the desired temperature range, the bulb was initially cooled to 4.2°K by a liquid helium bath, and then heated electrically above this point. The bulb was made of copper, to insure uniformity of temperature throughout it, and the resistors were placed directly on the outer surface of the bulb.

The pressure measuring device was a Wallace and Tierman gauge, type FA-145 (2 turn dial, 0-800 mm. Hg range). A .44 mm. inside diameter stainless steel capillary tube served as the connecting tube, and the gas used was helium.

The gauge was calibrated against a mercury manometer (assumed

correct) both before and after calibration of the resistors. There appeared a linear deviation with pressure which was regarded as a systematic error in the gauge and a correction for it was made in the subsequent calculations.

The volume of the gauge, v, was determined by comparison with a known volume. The value was

$$v = 10.4(1 + 1.4 \times 10^{-4}P) \pm .3 \text{ cm}^3$$

where P is the pressure in mm. of Hg. (This correction term accounts for the fact that the gauge had a bellows type pressure sensing element).

Since it was desired that V the volume of the bulb should be at least 230 cm^3. A 1 1/2" copper pipe, 10" long, sealed at the ends produced a volume calculated to be 273.4 $\pm$ .7 cm^3 at room temperature.

Because of the size of the dewar, it was necessary to have the capillary 48" long. This resulted in a calculated volume for the connecting tube of only .19 cm^3, well within the design criteria.

As liquid helium temperature (approximately 4.2°K) would be the lowest temperature used in the calibration, some means must be devised to thermally isolate the bulb from the bath, once it was in equilibrium with the bath, in order to raise it above this point. For this reason the bulb was suspended in a vacuum container which was to be immersed in the bath. The bulb support was a 3/8" O.D. (.01" wall thickness) stainless steel tube. This tube also extended up and out of the cryostat and served as the pumping line. An electrical heater of about 1500 ohms, consisting of 12 feet of .002" manganin wire (ℓ = 78.3 ohms/ft.) was wound around the bulb and glued there with G. E. 7031 varnish. The heater was necessary to raise the

temperature and to compensate for the resultant heat leak through the support (and to a much lesser extent, the heat leak due to radiation and conduction by any residual gas).

The resistors to be calibrated were inserted into small receptacles in the bulb. In order to avoid the relatively large electrical lead resistance, a three wire connection was made to each resistor. This, and a discussion of the low power A. C. bridge used, is given in the work by Reese and Tucker, and will not be presented here [34].

A schematic diagram of the completed system in shown in figure 7.

Gas Bulb Calibration Procedures

The gas bulb was filled with gaseous helium to about 790 mm. of Hg when the system was at liquid air temperature. The vacuum spaces were then pumped to approximately 10^{-7} Torr and the liquid helium space was filled.

The data accrual was quite simple. The procedure was to heat for a period of about 30 seconds, then turn off the heating power, and then observe the resistances come to equilibrium, which indicated temperature equilibrium. The pressures and resistance values were then recorded. The tendency for the temperature to drift downward, due to the heat leak, was compensated for by the heater.

The observations were taken over a pressure range of about 40-300 mm. of Hg, corresponding to temperatures of from 4 to 30 degrees. They were taken twice over the entire range, at about 2-4 mm. steps, to check reproductibility, and a third time over the lowest portion of the range where the resistors were the most sensitive. Seventy-three points were taken altogether.

After completion of this procedure, the bulb was allowed to come

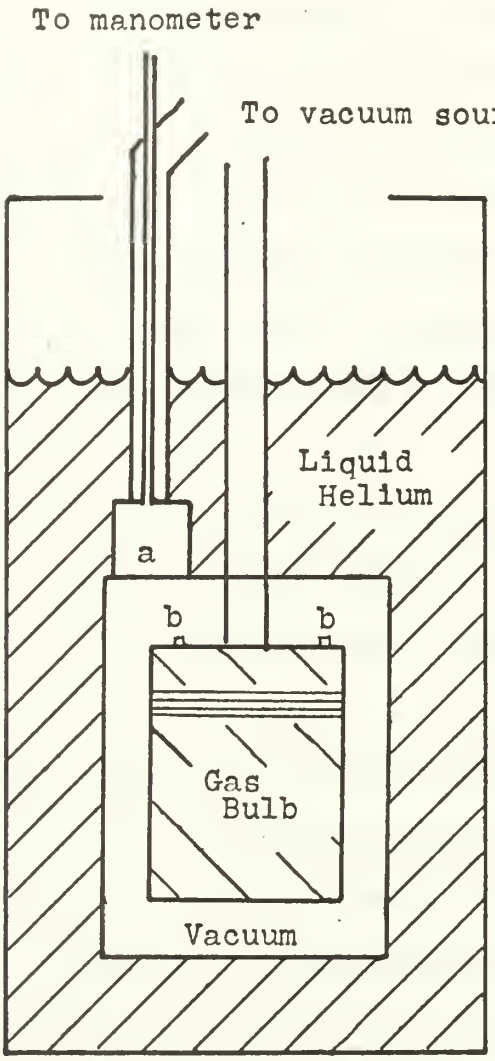

a. Vapor bulb

b. Resistors to be calibrated

Figure 7. Schematic of gas bulb thermometer.

to complete equilibrium with the liquid helium bath. Using the vapor pressure, the bath temperature was determined. This would later serve as a check on the accuracy of the calibrating procedures. The helium was then evaporated from the dewar and the space filled with liquid nitrogen (99.9% pure). The pressure in the gas bulb together with the known temperature of the nitrogen bath gave values of P_N and T_N which could then be used in equation A.9, and the pressures could be converted into temperatures.

Equation A.9 is here rewritten with a slight amplification of the terms.

A.10
$$\frac{P_N V_N}{T_N + B_N P_N} + \frac{P_N v}{T_r + B_r P_N} + \frac{P_N v'}{T_c + B_c P_N} = \frac{PV}{T + BP} + \frac{Pv}{T_r + B_r P} + \frac{Pv'}{T_c' + B_c' P}$$

where P_N is the pressure in the system when the bulb is at liquid nitrogen temperature, T_N is the liquid nitrogen temperature, V is the volume of the bulb at temperatures less than 30°K, and V_N is the volume of the bulb at T_N. The subscript r refers to ambient conditions in the laboratory, and the other symbols have the same meaning as before. Using published values for the thermal contraction of copper at the various temperatures, it is found that $V = 270.8 \pm .7$ cm^3 and $V_N = 273.0 \pm .7$ cm^3 [26]. For an estimate of the T_c's, a value of 145°K was assumed for T_c', and 108°K for T_c. These were obtained by assuming a linear temperature distribution along the capillary. This is sufficiently accurate as this part of the system is quite small. Values of the second virial coefficients were taken from Keeson;[22]

A.11 $\mathcal{B} = (.2453 - 6.2009/T)\ ^{\circ}K/mm\ of\ Hg$

$\mathcal{B}_N = .000163$

$\mathcal{B}_V = .000162$

$\mathcal{B}_c = .000179$

$\mathcal{B}_c' = .000186$.

Using the above in equation A.10 leads to an equation quadratic in . Solving that for T yields,

A.12 $$T = -\frac{b}{2} + \frac{1}{2}\sqrt{b^2 - 4a}$$

where $$a = -\beta P$$

$$b = \left(\frac{V}{C} - \alpha\right)P$$

$$c = P_N\left(\frac{V_N}{T_N + B_N P_N} + \frac{v}{T_V + B_V P_N} + \frac{v'}{T_c + B_c P_N}\right) - P\left(\frac{v}{T_V + B_V P} + \frac{v'}{T_c' + B_c' P}\right)$$

$$\alpha = .2453 \qquad \beta = 6.2009 .$$

Equation A.12 was programmed for the CDC 1604 digital computer.

The procedure discussed above gave only a pressure-resistance relationship until equation A.12 was solved. To obtain the desired temperature-resistance dependence, all the data was best fitted, in the least squares sense, by the computer to the following type of equation for each resistor;

A.13 $$T = \sum_{i=1}^{7} A_i' \left(\log_{10} R\right)^{m-i-1}$$

where the A_i's and the best fitted m (integers between 1 and 7) were determined. The values are presented at the end of this appendix, and the RMS deviation from this fitting is calculated to be .23%.

Calibration of the Thermometers below 4.2°K

For temperature determination from 1 to 5.2°K, the International Commission on Weights and Measures adopted the "1958 He^4 Vapor Pressure Scale of Temperatures" as the international standard [8,48]. Tables based on this scale give a conversion from vapor pressures to temperatures, hence the temperature can be ascertained from a reading of the vapor pressure alone.

For this lower temperature determination, it was decided to use a vapor bulb thermometer, rather than merely measuring the pressure above the bath since the latter procedure involves making corrections and assumptions of questionable validity.

Vapor bulb thermometery is performed by placing a container into the helium bath at the liquid level at which the temperature is desired to be known, and filling the container with gaseous helium until the gas condenses which indicates equilibrium between the liquid and gas phases at this pressure [42]. The pressure is then observed, and tables give the temperature directly.

For the actual construction of the bulb a small copper cylinder with a volume of approximately 2 cm^3 was connected by a 1/8' stainless tube to a mercury manometer and filling manifold. The bulb was mounted directly on top of the vacuum container, and connecting tube was brought outside of the cryostat enclosed in an evacuated tube (to prevent gas oscillations in the system [42]. See figure 7.

For the calibration, exchange gas was introduced into the vacuum space where the resistors were located, and the pressure above the bath was lowered in steps. The manometer readings were taken and the corresponding resistances were recorded. In all 32 points were

taken in the temperature range of from 2.4 to 4.2°K.

After conversion of the pressures into temperatures, the resistance values were related to the temperature by equation A.13.

Recalibration of the Thermometers

Inasmuch as the comparison experiment (Appendix B) indicated that a systematic error might be present in the temperature scale, the scale was reestablished. Also, in the initial calibrations, the vapor pressure and the gas bulb temperature scales (below and above 4.2°K) were independently determined with the result that there existed a slight discrepancy at their common temperatures. (Approximately .2% difference). Since it was desired to have a continuous scale over the entire range, the calibration was repeated insuring that the temperature overlap was consistant with both types of temperature determination. This was accomplished by using the liquid helium temperatures, as determined by vapor pressures, as the fixed points for the gas bulb calibration rather than the liquid nitrogen point. As a check as to the precision of this method, the predicted liquid nitrogen temperature was only .3°K different from the assumed value of 77.35°K, a difference of only .23%.

The equipment and procedures were the same as outlined earlier. A total of 99 points were taken over the entire range, varying the intervals so that a uniform coverage was obtained. The gauge volume was again experimentally determined, and was within 3% of the original measurement. The gauge was likewise recalibrated against a mercury manometer twice.

The resistance values were related to the temperature by use of equation A.13.

Accuracy of the Calibration

In the temperature range below 4.2°K where the vapor bulb thermometer was employed, the only significant source of error in the temperature determination was the reading of the manometer. It could be read to within .001 cm of Hg with reproducibility of .003 cm. of Hg. This results in a maximum uncertainty in the temperature for this range of 3 millidegrees.

For the gas bulb calibration, which covered the temperature range of from 4.2 to 30°K, the following effects were considered to ascertain an estimate of the error;

(a) The fixed temperature point.

The calibration over the entire range is very sensitive to any errors in the determination of the fixed temperature point which essentially sets a value for the right hand side of equation A.12. To determine this parameter, six independent observations of the temperature were made, by vapor bulb methods, at the liquid helium bath temperature, and the pressure associated with each recorded. The fixed point was taken to be the average of these data. The resulting error in the temperature determination over the entire range due to this was estimated to be at most .003 degrees.

(b) Errors in the measurement of volumes.

Since the bulb's volume was much greater than the other volumes in the system, the temperature is essentially linear in the pressure. This tends to make any error in the measurements of the volumes self compensating, and their net contribution to the error in the calibration is negligible.

(c) Thermalmolecular correction.

Following Roberts and Sydoriak, the thermalmolecular correction is .004° at the low end of the temperature scale (4.2°K), and negligible above 7°K [37]. This systematic error could have been corrected for, but was not in view of the existing larger errors which will be discussed below.

(d) Pressure measurement.

The pressure measuring gauge readings were compared with those of a mercury manometer both before and after the resistor calibration. This comparison was made stepwise going up in pressures, since this was the way data were taken, to include any hysteresis of the gauge's bellows as part of the correction. The gauge was determined to have a linear error as a function of pressure, that is, the deviation was consistently high at the higher pressures, and low at the lower ones. The data were corrected for the presence of this systematic error. The statistical uncertainty of this correction is entirely compatible with the precision to which the gauge could be read, about .1 mm. Due to the uncertainty in the pressure determination, a possible error of .01° exists throughout the temperature range.

Other sources of error, such as those considered by Beattie, and those due to the uncertainty of the values of the virial coefficients, accuracy of the mercury manometer, etc., were considered to be insignificant compared with the ones discussed above [5].

Once the temperature scale was established, there exists the necessity of relating the resistance values of the resistors with the temperatures. This introduces another possible reading error which amounts to .1% over the entire range. However it is felt that due to

the insensitivity of the resistors at the higher temperatures, a more realistic value of .3% should be assigned there. After the resistance-temperature relation had been established by equation A.13, it was possible to assign the maximum temperature differences these errors would introduce, .0015° at 2.5 and .03° at the highest temperatures. It is also noted that to use the resistors as thermometer, another reading error of this size could exist.

Summarizing all of the above, and recognizing that the fitted relation between the temperature and the sample thermometer resistance values contains an uncertainty, it is felt that the temperature determination by use of the resistors was accurate to within .5% of the absolute temperature.

As an estimate of the reproducibility and precision of the calibration, the RMS deviation of the actual points from the fitted resistance-temperature was used. This amounted to .23%, and appeared to be randomized. Hence the statistical scatter of the calibration points from the fitted relation was well within the estimated errors of the procedure.

Parameters for the temperature-resistance fitted relation

$$T = \sum_{i=1}^{7} A_i (\log_{10} R)^{n-i-1}.$$

	Thermometer		
	Shield (4.2-30°K)	Shield (2.4-4.2°K)	Sample (2.4-30°K)
n	6	6	4
A_1	$.81986 \times 10^{-1}$	$-.11574 \times 10^{-1}$	$-.24787 \times 10^{0}$
A_2	$.65400 \times 10^{-2}$	$.66904 \times 10^{-1}$	$.32888 \times 10^{1}$
A_3	$-.50749 \times 10^{1}$	$.25718 \times 10^{-1}$	$-.10029 \times 10^{2}$
A_4	$.17961 \times 10^{2}$	$.10939 \times 10^{0}$	$-.36394 \times 10^{2}$
A_5	$.14366 \times 10^{2}$	$-.27080 \times 10^{1}$	$.25491 \times 10^{3}$
A_6	$-.15249 \times 10^{3}$	$-.69149 \times 10^{1}$	$-.45361 \times 10^{3}$
A_7	$.19880 \times 10^{3}$	$.38145 \times 10^{2}$	$.36772 \times 10^{3}$
% RMS Deviation	.20	.00	.23

APPENDIX B - Comparison Experiment

There has been considerable discussion about the need for, and choice of, a suitable calorimetric standard in the temperature range below 20°K [53]. Because of the large number of specific heat determinations for copper, its available purity, and other reasons, there is much support for its choice as such a standard. At the same time that this experiment was being performed, Martin reported the specific heat of a cast 99.999% pure copper sample in the temperature range of this experiment [30]. He asserts that his results are accurate to better than 1%, which implys a temperature determination to within .35% accuracy.

To ascertain an estimate on the accuracy of the temperature scale used in the present experiment, it was decided to duplicate Martin's measurements. A single crystal copper sample of 99.9995% purity was obtained (Semi-Elements, Inc.), and was etched with nitric acid to a size which was compatible with the calorimeter. The resulting sample was a 2¼" by 9/16" rod with a mass of 83.181 grams. Heat capacity measurements were performed on this sample, in the same manner as for the polyethylene samples, over the temperature range 4.5 to 30°K.

In performing these measurements, the only experimental procedural differences from the polyethylene runs were that the amount of heat introduced for the temperature steps was considerably less, and the equilibrium times were much shorter, due to the differing heat capacity and thermal conductance. Three complete sets of measurements were obtained over the aforementioned temperature range, resulting in a total of 119 data points.

After smoothing the data by least squares fitting it to a seven parameter equation (equation 3.2) and correcting for the heat capacity of the addenda, the results were compared with those of Martin. They matched fairly well at the low temperature end, this work being about 2% lower, and excellent agreement was obtained at the highest temperatures where no difference was found. However Martin's results were over 5% higher at the midpoint, 17°K. The differences along the scale were not random but showed a clear divergence up to a maximum, and then converged to zero at the highest temperatures. This type of deviation can most easily be explained as some sort of systematic error in the determination of either temperature scale, or possibly a drift of the resistance values of the thermometers. Martin discounts this latter possibility in his work by repeated checks against both vapor bulb and gas bulb thermometery. In the present work nearly every time the system was at equilibrium with the helium bath, the thermometers were checked against the vapor pressure temperature of the bath. On the basis of this, it is felt that there was no resistance drift of the thermometers used here at least at the low temperatures.

The size of the maximum difference in the two sets of results is quite large, but it should be pointed out that at 17°K an error in the temperature determination of only 1.3% (.2°) would explain the difference. This value of error is outside of the estimated error in the temperature scale used here, however, and so it was decided that a recalibration of the thermometers would be performed at the conclusion of the specific heat measurements on polyethylene (the copper data were taken about half way through the polyethylene work). It was felt that with the low temperature techniques acquired

by this experimenter that a more precise calibration might be achieved. The recalibration is discussed in Appendix A.

After the recalibration was performed, the heat capacity data for copper were recalculated, and again compared with the results of Martin. The same relative deviation persisted, however it was approximately halved at the 17°K point (2.6% low). At the highest temperatures investigated, 30°K, the results were again the same as Martin's, but the same 2% difference was still present at 5°K.

The new calibration was decided to be the more accurate and was used based on the following considerations. First the agreement with Martin's copper data was better. Next the recalibration was performed after this experimenter had considerably more experience with the low temperature techniques, and was able to look for small systematic errors which may have been overlooked the first time. Lastly this calibration was continuous over the range 2.4 to 30°K which was highly desirable (see Appendix A).

At the conclusion of this work, Alhers published specific heat data on copper over essentially the same temperature range as that under consideration [1]. His work compares very well with that of Martin, but has the same relative deviation from this work. For comparison, the present copper specific heat data are presented below along with that of both Martin and Alhers. Additionally the parameters for the fitted curve equation (3.2) are given, along with its o/o RMS deviation from the actual data points, (.69%).

Parameters for the specific heat-temperature fitted relation

$C = \sum_{i=1}^{7} A_i T^{i-1}$ (C in mj/°K-gm). For T between 2.4 and 30°K.

A_1	$-.12463X10^{0}$
A_2	$.96209X10^{-1}$
A_3	$-.23948X10^{-1}$
A_4	$.41835X10^{-2}$
A_5	$-.26648X10^{-3}$
A_6	$.10385X10^{-4}$
A_7	$-.14265X10^{-6}$
% RMS Deviation	.69

Molecular weight of copper 63.57 gms/mole

COMPARISON OF SPECIFIC HEAT OF COPPER

SPECIFIC HEATS IN MJ/0K/GM

TEMPERATURE	C(TUCKER)	C(MARTIN)	C(ALHERS)
5.0	.1443	.1475	.1484
6.0	.2229	.2265	.2275
7.0	.3283	.3334	.3339
8.0	.4657	.4729	.4725
9.0	.6403	.6505	.6488
10.0	.8573	.8718	.8690
11.0	1.1226	1.1444	1.1399
12.0	1.4430	1.4737	1.4690
13.0	1.8266	1.8708	1.8647
14.0	2.2823	2.3409	2.3356
15.0	2.8205	2.8960	2.8910
16.0	3.4521	3.5440	3.5400
17.0	4.1892	4.3006	4.2917
18.0	5.0439	5.1619	5.1548
19.0	6.0286	6.1542	6.1388
20.0	7.1546	7.2829	7.2549
21.0	8.4324	8.5537	8.5193
22.0	9.8702	9.9695	*
23.0	11.4734	11.5367	*
24.0	13.2436	13.2685	*
25.0	15.1772	15.1584	*
26.0	17.2649	17.1997	*
27.0	19.4898	19.3727	*
28.0	21.8264	21.6576	*
29.0	24.2389	24.0413	*
30.0	26.6797	26.5238	*

* INDICATES NO DATA

MARLEX 1

SPECIFIC HEATS IN MJ/OK/GM

TEMPERATURE	C
2.597	.18796
2.604	.19134
2.587	.19166
2.741	.23133
2.768	.23560
2.754	.23643
2.896	.27448
2.913	.28187
2.934	.28523
3.048	.32351
3.074	.33065
3.098	.33663
3.200	.37506
3.234	.38555
3.258	.39376
3.379	.44463
3.433	.45855
3.415	.46099
3.594	.52877
3.618	.52938
3.617	.53548
3.808	.61506
3.804	.63022
3.819	.63708
3.998	.71218
4.003	.72960
4.046	.75817
4.196	.82776
4.210	.85138
4.271	.88733
4.326	.92379
4.340	.93608
4.366	.96433
4.419	.98215
4.490	1.04819
4.517	1.05959
4.539	1.07225
4.637	1.13612
4.635	1.14261
4.673	1.16034
4.696	1.18922
4.774	1.21738
4.824	1.29738
4.845	1.30108
4.863	1.32905

MARLEX 1

SPECIFIC HEATS IN MJ/OK/GM

TEMPERATURE	C
4.970	1.39622
4.991	1.44958
5.011	1.45996
5.100	1.54250
5.135	1.61394
5.210	1.64436
5.229	1.66338
5.304	1.74434
5.355	1.79458
5.418	1.84677
5.468	1.91434
5.520	1.96849
5.604	2.06463
5.637	2.08688
5.686	2.16203
5.746	2.21610
5.771	2.27986
5.911	2.42215
5.930	2.42923
6.086	2.62558
5.992	2.62725
6.181	2.75895
6.233	2.81262
6.236	2.84967
6.513	3.19788
6.532	3.24379
6.549	3.30149
6.572	3.31813
6.868	3.72186
6.905	3.82183
6.953	3.85513
6.892	3.89666
7.178	4.22355
7.204	4.23521
7.229	4.32056
7.344	4.50184
7.456	4.63985
7.535	4.83053
7.541	4.85262
7.711	4.97886
7.847	5.41547
7.909	5.51952
7.944	5.53639
8.157	5.94872
8.208	6.12060

MARLEX 1

SPECIFIC HEATS IN MJ/OK/GM

TEMPERATURE	C
8.277	6.29253
8.437	6.53970
8.671	7.00062
8.623	7.19002
8.773	7.29157
8.985	7.70739
9.075	7.98402
9.077	8.03411
9.353	8.54090
9.415	8.88594
9.424	8.93725
9.610	9.34961
9.820	9.74374
9.847	9.97924
9.990	10.61803
10.265	11.22138
10.331	11.48649
10.604	12.30049
10.834	12.99738
10.892	13.17960
11.148	14.03310
11.339	14.67437
11.400	14.93354
11.644	15.82448
11.786	16.29977
11.949	16.91263
12.162	17.62685
12.198	17.79657
12.832	20.28792
12.859	20.48844
13.239	22.24001
13.642	23.72455
13.635	23.74350
13.856	24.79318
14.326	26.70627
14.343	26.93295
14.563	27.92274
14.988	29.89960
14.973	31.75482
15.371	31.86838
15.634	32.10680
16.320	37.06861
17.374	42.64875
17.488	43.70005
17.819	45.38054

MARLEX 1

SPECIFIC HEATS IN MJ/OK/GM

TEMPERATURE	C
18.430	48.82613
18.466	49.36476
18.875	51.37767
19.274	54.50185
19.555	56.01417
19.799	57.71516
20.105	59.66975
20.724	63.97106
20.884	65.13815
21.133	68.59212
21.667	71.31811
21.910	71.80872
22.468	77.27470
23.028	80.64122
22.828	81.65808
23.499	85.04005
23.845	88.50399
24.186	91.55677
24.980	95.85445
25.001	98.14700
25.292	100.16830
26.191	106.23490
26.578	115.46438
27.159	118.91252
27.572	121.90134
28.825	132.66855

MARLEX 2

SPECIFIC HEATS IN MJ/OK/GM

TEMPERATURE	C
4.349	1.10836
4.375	1.15563
4.373	1.15943
4.538	1.26999
4.540	1.28241
4.568	1.31700
4.703	1.41884
4.740	1.46093
4.762	1.50724
4.881	1.60343
4.948	1.66051
4.967	1.70458
5.092	1.82800
5.170	1.91897
5.187	1.96224
5.301	2.05350
5.390	2.17302
5.484	2.22102
5.412	2.25201
5.606	2.44090
5.670	2.51030
5.645	2.53578
5.850	2.77896
5.859	2.78156
5.897	2.89658
6.078	3.09759
6.197	3.28717
6.165	3.31436
6.378	3.60245
6.454	3.75170
6.595	3.93908
6.718	4.14388
6.770	4.29967
6.952	4.57285
7.030	4.73857
7.118	4.93654
7.315	5.26753
7.330	5.29696
7.489	5.69568
7.642	5.90489
7.698	6.04339
7.875	6.53743
7.990	6.69330
8.098	6.94474
8.338	7.47455

MARLEX 2

SPECIFIC HEATS IN MJ/OK/GM

TEMPERATURE	C
8.612	8.36381
8.673	8.37944
8.720	8.42132
9.164	9.63058
9.337	10.13203
9.447	10.62664
9.711	11.61380
9.907	11.85851
10.000	12.28690
10.314	13.08954
10.456	13.67324
10.534	14.10426
10.860	15.03178
11.017	15.61562
11.098	16.19879
11.391	16.97032
11.600	17.80159
11.694	18.33617
11.938	19.13534
12.195	20.23688
12.315	20.92201
12.493	21.41557
12.797	22.72404
12.961	23.71420
13.066	23.89595
13.413	25.43271
13.701	26.84314
13.660	26.95160
14.144	29.02634
14.353	30.01182
14.422	30.75287
14.929	32.89604
15.030	33.22668
15.236	34.73176
15.738	37.14855
15.784	37.24379
16.060	39.29161
16.573	41.48706
16.596	42.02919
16.911	44.06952
17.397	46.24928
17.448	46.91189
17.827	49.84552
18.145	50.75218
18.345	52.51535

MARLEX 2

SPECIFIC HEATS IN MJ/OK/GM

TEMPERATURE	C
18.832	55.59494
18.789	55.66262
19.311	58.92028
19.688	62.09741
19.790	62.71279
20.324	66.22665
20.554	68.59343
20.833	71.12623
21.507	73.83893
21.511	75.11742
21.938	78.73929
22.729	82.89937
22.647	84.30054
23.086	88.27922
23.871	92.26345
23.844	96.20608
24.266	96.79725
24.965	102.41275
25.217	104.56977
25.469	110.32250
26.118	112.90491
26.716	117.49972
26.707	119.71567
27.999	131.33693
28.399	131.63365
28.601	132.40289
29.244	137.68334

LOW DENSITY

SPECIFIC HEATS IN MJ/OK/GM

TEMPERATURE	C
2.521	.28781
2.533	.29686
2.579	.31867
2.621	.33245
2.655	.35445
2.695	.37404
2.731	.38825
2.780	.41757
2.816	.42907
2.851	.44835
2.908	.47711
2.941	.50078
2.978	.51675
3.063	.57180
3.097	.57700
3.088	.59378
3.241	.65976
3.251	.67721
3.266	.69384
3.454	.81479
3.449	.81595
3.440	.82114
3.645	.96564
3.648	.96623
3.657	.97461
3.843	1.13362
3.851	1.14367
3.863	1.14469
4.052	1.33429
4.061	1.33820
4.064	1.34516
4.278	1.57952
4.328	1.61775
4.318	1.62234
4.335	1.63967
4.474	1.81021
4.498	1.81792
4.497	1.84558
4.508	1.86155
4.642	2.03621
4.682	2.06809
4.706	2.13112
4.831	2.30063
4.888	2.38673
4.932	2.46734

LOW DENSITY

SPECIFIC HEATS IN MJ/OK/GM

TEMPERATURE	C
5.034	2.63293
5.116	2.74904
5.140	2.79630
5.189	2.88276
5.245	2.96659
5.360	3.19051
5.382	3.21864
5.450	3.36224
5.470	3.36955
5.615	3.64384
5.634	3.68241
5.712	3.83001
5.713	3.85035
5.893	4.22231
5.916	4.27282
5.980	4.32430
5.992	4.45900
6.209	4.91476
6.235	4.95730
6.277	5.03374
6.303	5.10324
6.550	5.69680
6.575	5.76155
6.592	5.78959
6.644	6.00095
6.904	6.59770
6.928	6.63617
6.922	6.65371
7.268	7.52172
7.263	7.56141
7.287	7.61844
7.625	8.57451
7.669	8.71615
8.024	9.80153
8.082	9.98707
8.405	11.06141
8.460	11.21426
8.505	11.36980
8.815	12.46119
8.899	12.75976
8.933	12.86687
9.231	13.96903
9.361	14.44571
9.387	14.58159
9.661	15.61894

LOW DENSITY

SPECIFIC HEATS IN MJ/OK/GM

TEMPERATURE	C
9.884	16.52142
9.894	16.57931
10.127	17.59983
10.464	18.91642
10.452	18.95116
10.639	19.73098
11.038	21.57511
11.064	21.69968
11.194	22.29614
11.631	24.39704
11.669	24.42918
11.788	25.18032
12.229	27.30692
12.276	27.65680
12.410	28.33392
12.845	30.68352
12.901	30.86788
13.063	31.55914
13.515	34.28889
13.576	34.61570
13.767	35.76025
14.245	38.38456
14.311	38.66656
14.528	39.96585
15.022	42.96486
15.094	43.32534
15.340	44.96633
15.862	48.09940
15.940	48.47511
16.220	50.30252
16.758	53.82994
16.845	54.36106
17.137	56.28382
17.700	59.96677
17.785	60.70527
18.713	67.33329
18.777	67.69524
19.002	69.52506
19.788	75.32322
19.860	76.15117
19.986	76.79421
20.904	84.22005
20.958	84.50975
21.034	85.05182
22.047	92.92935

LOW DENSITY

SPECIFIC HEATS IN MJ/OK/GM

TEMPERATURE	C
22.118	94.18537
22.118	94.42999
23.228	103.33531
23.336	103.43852
23.211	103.96273
24.385	113.53377
24.352	115.23389
24.560	116.08967
25.490	124.87124
25.557	125.00688
25.776	125.96857
26.735	133.83623
26.654	134.54346
26.992	135.14483
27.869	140.81310
27.939	143.93052
28.215	145.08745
29.122	154.61557
29.283	156.00964
29.038	161.87336

THE 100 0/0 CRYSTALINE SAMPLE

HEAT CAPACITIES IN MJ/0K/GM

TEMPERATURE	C ACTUAL	TARASOV C	PER CENT DIFFERENCE
2.5	.124	.123	.9
3.0	.211	.213	-.7
3.5	.335	.337	-.9
4.0	.501	.504	-.6
4.5	.715	.717	-.3
5.0	.984	.984	.0
5.5	1.313	1.310	.3
6.0	1.708	1.700	.5
6.5	2.174	2.162	.5
7.0	2.715	2.700	.6
7.5	3.337	3.321	.5
8.0	4.045	4.030	.4
8.5	4.842	4.832	.2
9.0	5.732	5.735	-.1
9.5	6.719	6.742	-.3
10.0	7.805	7.858	-.7
10.5	8.994	9.087	-1.0
11.0	10.288	10.433	-1.4
11.5	11.689	11.898	-1.8
12.0	13.197	13.485	-2.2
12.5	14.815	15.195	-2.6
13.0	16.543	17.029	-2.9
13.5	18.381	18.985	-3.3
14.0	20.330	21.064	-3.6
14.5	22.389	23.263	-3.9
15.0	24.558	25.581	-4.2
15.5	26.836	28.013	-4.4
16.0	29.221	30.557	-4.6
16.5	31.713	33.210	-4.7
17.0	34.310	35.966	-4.8
17.5	37.010	38.822	-4.9
18.0	39.812	41.773	-4.9
18.5	42.714	44.815	-4.9
19.0	45.715	47.942	-4.9
19.5	48.813	51.151	-4.8
20.0	52.007	54.435	-4.7
20.5	55.295	57.792	-4.5
21.0	58.677	61.215	-4.3
21.5	62.152	64.701	-4.1
22.0	65.720	68.245	-3.8
22.5	69.381	71.844	-3.5
23.0	73.138	75.492	-3.2
23.5	76.990	79.187	-2.9
24.0	80.942	82.924	-2.4
24.5	84.996	86.701	-2.0
25.0	89.156	90.513	-1.5
25.5	93.429	94.358	-1.0
26.0	97.821	98.233	-.4
26.5	102.339	102.135	.2
27.0	106.994	106.061	.9
50.0	332.800	290.367	12.8
100.0	682.400	644.550	5.5
150.0	942.900	920.149	2.4
200.0	1197.000	1117.313	6.7

THE MARLEX ONE SAMPLE

HEAT CAPACITIES IN MJ/OK/GM

TEMPERATURE	C ACTUAL	TARASOV C	PER CENT DIFFERENCE
2.5	.172	.171	.5
3.0	.303	.303	-.0
3.5	.487	.490	-.5
4.0	.735	.739	-.5
4.5	1.053	1.057	-.3
5.0	1.449	1.448	.1
5.5	1.928	1.920	.4
6.0	2.495	2.478	.7
6.5	3.154	3.127	.8
7.0	3.909	3.875	.9
7.5	4.761	4.725	.8
8.0	5.714	5.682	.6
8.5	6.768	6.749	.3
9.0	7.926	7.932	-.1
9.5	9.187	9.231	-.5
10.0	10.553	10.647	-.9
10.5	12.023	12.184	-1.3
11.0	13.597	13.841	-1.8
11.5	15.275	15.618	-2.2
12.0	17.057	17.515	-2.7
12.5	18.943	19.530	-3.1
13.0	20.931	21.663	-3.5
13.5	23.021	23.911	-3.9
14.0	25.213	26.272	-4.2
14.5	27.506	28.742	-4.5
15.0	29.899	31.319	-4.7
15.5	32.392	33.998	-5.0
16.0	34.985	36.776	-5.1
16.5	37.676	39.648	-5.2
17.0	40.465	42.611	-5.3
17.5	43.353	45.659	-5.3
18.0	46.338	48.789	-5.3
18.5	49.420	51.995	-5.2
19.0	52.600	55.274	-5.1
19.5	55.876	58.621	-4.9
20.0	59.248	62.031	-4.7
20.5	62.717	65.501	-4.4
21.0	66.281	69.026	-4.1
21.5	69.940	72.602	-3.8
22.0	73.693	76.226	-3.4
22.5	77.539	79.893	-3.0
23.0	81.476	83.601	-2.6
23.5	85.505	87.346	-2.2
24.0	89.622	91.125	-1.7
24.5	93.825	94.934	-1.2
25.0	98.112	98.772	-.7
25.5	102.479	102.634	-.2
26.0	106.923	106.520	.4
26.5	111.439	110.426	.9
27.0	116.021	114.350	1.4
50.0	332.800	296.206	11.0
100.0	682.400	646.873	5.2
150.0	942.900	921.362	2.3
200.0	1197.000	1118.064	6.6

THE MARLEX TWO SAMPLE

HEAT CAPACITIES IN MJ/OK/GM

TEMPERATURE	C ACTUAL	TARASOV C	PER CENT DIFFERENCE
2.5	*	.201	*
3.0	*	.357	*
3.5	*	.582	*
4.0	*	.881	*
4.5	1.249	1.261	-1.0
5.0	1.735	1.729	.4
5.5	2.315	2.288	1.2
6.0	2.995	2.947	1.6
6.5	3.778	3.711	1.8
7.0	4.666	4.584	1.8
7.5	5.662	5.573	1.6
8.0	6.765	6.679	1.3
8.5	7.977	7.907	.9
9.0	9.297	9.258	.4
9.5	10.724	10.733	-.1
10.0	12.258	12.332	-.6
10.5	13.898	14.054	-1.1
11.0	15.643	15.898	-1.6
11.5	17.490	17.863	-2.1
12.0	19.440	19.947	-2.6
12.5	21.491	22.148	-3.1
13.0	23.642	24.462	-3.5
13.5	25.891	26.886	-3.8
14.0	28.240	29.417	-4.2
14.5	30.685	32.051	-4.4
15.0	33.229	34.784	-4.7
15.5	35.869	37.612	-4.9
16.0	38.606	40.531	-5.0
16.5	41.439	43.536	-5.1
17.0	44.370	46.623	-5.1
17.5	47.398	49.787	-5.0
18.0	50.522	53.024	-5.0
18.5	53.744	56.330	-4.8
19.0	57.062	59.701	-4.6
19.5	60.476	63.131	-4.4
20.0	63.985	66.617	-4.1
20.5	67.588	70.155	-3.8
21.0	71.283	73.742	-3.4
21.5	75.067	77.372	-3.1
22.0	78.936	81.044	-2.7
22.5	82.887	84.753	-2.3
23.0	86.913	88.497	-1.8
23.5	91.007	92.272	-1.4
24.0	95.161	96.076	-1.0
24.5	99.365	99.905	-.5
25.0	103.607	103.758	-.1
25.5	107.872	107.631	.2
26.0	112.144	111.523	.6
26.5	116.405	115.432	.8
27.0	120.633	119.355	1.1
50.0	332.800	299.732	9.9
100.0	682.400	648.275	5.0
150.0	942.900	922.095	2.2
200.0	1197.000	1118.518	6.6

THE LOW DENSITY SAMPLE

HEAT CAPACITIES IN MJ/OK/GM

TEMPERATURE	C ACTUAL	TARASOV C	PER CENT DIFFERENCE
2.5	.288	.288	.0
3.0	.523	.520	.6
3.5	.855	.855	-.1
4.0	1.298	1.304	-.5
4.5	1.865	1.871	-.3
5.0	2.566	2.564	.1
5.5	3.405	3.386	.6
6.0	4.386	4.345	.9
6.5	5.510	5.448	1.1
7.0	6.776	6.697	1.2
7.5	8.182	8.098	1.0
8.0	9.724	9.651	.7
8.5	11.397	11.356	.4
9.0	13.197	13.210	-.1
9.5	15.118	15.209	-.6
10.0	17.153	17.349	-1.1
10.5	19.298	19.624	-1.7
11.0	21.546	22.028	-2.2
11.5	23.892	24.554	-2.8
12.0	26.331	27.195	-3.3
12.5	28.860	29.945	-3.8
13.0	31.473	32.798	-4.2
13.5	34.169	35.746	-4.6
14.0	36.945	38.784	-5.0
14.5	39.799	41.906	-5.3
15.0	42.732	45.106	-5.6
15.5	45.742	48.378	-5.8
16.0	48.832	51.716	-5.9
16.5	52.002	55.117	-6.0
17.0	55.255	58.575	-6.0
17.5	58.592	62.085	-6.0
18.0	62.017	65.643	-5.8
18.5	65.532	69.246	-5.7
19.0	69.141	72.888	-5.4
19.5	72.845	76.568	-5.1
20.0	76.647	80.280	-4.7
20.5	80.549	84.022	-4.3
21.0	84.551	87.791	-3.8
21.5	88.651	91.584	-3.3
22.0	92.848	95.399	-2.7
22.5	97.137	99.233	-2.2
23.0	101.511	103.083	-1.5
23.5	105.961	106.948	-.9
24.0	110.476	110.826	-.3
24.5	115.038	114.714	.3
25.0	119.628	118.612	.8
25.5	124.222	122.517	1.4
26.0	128.791	126.429	1.8
26.5	133.300	130.345	2.2
27.0	137.710	134.265	2.5
50.0	332.800	310.235	6.8
100.0	682.400	652.453	4.4
150.0	942.900	924.277	2.0
200.0	1197.000	1119.869	6.4

THE 0 0/0 CRYSTALINE (AMORPHOUS) SAMPLE

HEAT CAPACITIES IN MJ/OK/GM

TEMPERATURE	C ACTUAL	TARASOV C	PER CENT DIFFERENCE
2.5	.427	.428	-.2
3.0	.788	.781	1.0
3.5	1.296	1.295	.1
4.0	1.974	1.983	-.4
4.5	2.841	2.851	-.3
5.0	3.908	3.904	.1
5.5	5.179	5.148	.6
6.0	6.658	6.590	1.0
6.5	8.341	8.235	1.3
7.0	10.222	10.089	1.3
7.5	12.292	12.152	1.1
8.0	14.542	14.421	.8
8.5	16.959	16.891	.4
9.0	19.531	19.552	-.1
9.5	22.244	22.394	-.7
10.0	25.084	25.403	-1.3
10.5	28.040	28.565	-1.9
11.0	31.097	31.866	-2.5
11.5	34.246	35.291	-3.1
12.0	37.475	38.827	-3.6
12.5	40.776	42.460	-4.1
13.0	44.140	46.177	-4.6
13.5	47.563	49.967	-5.1
14.0	51.041	53.819	-5.4
14.5	54.570	57.723	-5.8
15.0	58.151	61.672	-6.1
15.5	61.783	65.655	-6.3
16.0	65.471	69.668	-6.4
16.5	69.216	73.704	-6.5
17.0	73.025	77.756	-6.5
17.5	76.903	81.822	-6.4
18.0	80.856	85.895	-6.2
18.5	84.891	89.974	-6.0
19.0	89.015	94.053	-5.7
19.5	93.234	98.132	-5.3
20.0	97.553	102.207	-4.8
20.5	101.975	106.277	-4.2
21.0	106.502	110.339	-3.6
21.5	111.133	114.393	-2.9
22.0	115.864	118.437	-2.2
22.5	120.685	122.470	-1.5
23.0	125.584	126.492	-.7
23.5	130.541	130.501	.0
24.0	135.533	134.498	.8
24.5	140.527	138.481	1.5
25.0	145.481	142.451	2.1
25.5	150.348	146.408	2.6
26.0	155.068	150.351	3.0
26.5	159.569	154.280	3.3
27.0	163.770	158.195	3.4
50.0	332.800	327.092	1.7
100.0	682.400	659.158	3.4
150.0	942.900	927.779	1.6
200.0	1197.000	1122.037	6.3

Parameters for the specific heat-temperature fitted relation

$$C = \sum_{i=1}^{7} A_i T^{i-1}$$ (C in mj/°K-gm for samples; mj/°K for addenda).

	100% (2.4-30°K)	Marlex I (2.4-30°K)	Marlex II (4.5-30°K)	Low Density (2.4-30°K)	0% (2.4-30°K)	Addenda (2.4-30°K)
A_1	$.35535 \times 10^{-1}$	$-.74812 \times 10^{-1}$	$-.44902 \times 10^{0}$	$-.33979 \times 10^{0}$	$-.65920 \times 10^{0}$	$-.11461 \times 10^{1}$
A_2	$-.24596 \times 10^{-1}$	$.10593 \times 10^{0}$	$.30654 \times 10^{0}$	$.41941 \times 10^{0}$	$.79698 \times 10^{0}$	$.11992 \times 10^{1}$
A_3	$.68702 \times 10^{-2}$	$-.58592 \times 10^{-1}$	$-.11611 \times 10^{0}$	$-.21582 \times 10^{0}$	$-.40503 \times 10^{0}$	$-.38694 \times 10^{0}$
A_4	$.62851 \times 10^{-2}$	$.25313 \times 10^{-1}$	$.38541 \times 10^{-1}$	$.71023 \times 10^{-1}$	$.12599 \times 10^{0}$	$.80686 \times 10^{-1}$
A_5	$.27844 \times 10^{-3}$	$-.12849 \times 10^{-2}$	$-.23583 \times 10^{-2}$	$-.50405 \times 10^{-2}$	$-.95559 \times 10^{-2}$	$-.55576 \times 10^{-2}$
A_6	$-.20717 \times 10^{-4}$	$.33102 \times 10^{-4}$	$.71612 \times 10^{-4}$	$.16239 \times 10^{-3}$	$.31782 \times 10^{-3}$	$.19714 \times 10^{-3}$
A_7	$.33088 \times 10^{-6}$	$-.34693 \times 10^{-6}$	$-.86571 \times 10^{-6}$	$-.19752 \times 10^{-5}$	$-.39327 \times 10^{-5}$	$-.25661 \times 10^{-5}$
% RMS Deviation	-	1.52	1.01	1.09	-	1.70

INITIAL DISTRIBUTION LIST

		No. Copies
1.	Defense Documentation Center Cameron Station Alexandria, Virginia 22314	20
2.	Library U.S. Naval Postgraduate School Monterey, California 93940	2
3.	Ordnance Systems Command Headquarters Department of the Navy Washington, D.C.	1
4.	Professor William Reese Physics Department U.S. Naval Postgraduate School Monterey, California 93940	5
5.	LCDR James E. Tucker Box 1362 U.S. Naval Postgraduate School Monterey, California 93940	1

DOCUMENT CONTROL DATA - R&D

(Security classification of title, body of abstract and indexing annotation must be entered when the overall report is classified)

1. ORIGINATING ACTIVITY *(Corporate author)*
U.S. Naval Postgraduate School
Monterey, California 93940

2a. REPORT SECURITY CLASSIFICATION
UNCLASSIFIED

2b. GROUP

3. REPORT TITLE
HEAT CAPACITY MEASUREMENTS ON POLYETHYLENE IN THE TEMPERATURE RANGE OF 2.4 TO 30°K

4. DESCRIPTIVE NOTES *(Type of report and inclusive dates)*
Thesis, Ph.D., May 1966

5. AUTHOR(S) *(Last name, first name, initial)*
Tucker, James Earl, LCDR, USN

6. REPORT DATE	7a. TOTAL NO. OF PAGES	7b. NO. OF REFS
May 1966	108	53

8a. CONTRACT OR GRANT NO.

b. PROJECT NO.

c.

d.

9a. ORIGINATOR'S REPORT NUMBER(S)

9b. OTHER REPORT NO(S) *(Any other numbers that may be assigned this report)*

10. AVAILABILITY/LIMITATION NOTICES
[redacted]. This document has been approved for public release and sale; its distribution is unlimited.

11. SUPPLEMENTARY NOTES

12. SPONSORING MILITARY ACTIVITY
Ordnance Systems Command Hdqrs.
Navy Department
Washington, D.C.

13. ABSTRACT

Specific heat measurements on three samples of polyethylene, differing only in density, were made in the temperature range of 2.4 to 30°K. A definite density dependence was noted for the specific heat in this temperature interval which allowed extrapolation of the data to completely crystalline and completely amorphous cases. At the lowest temperatures, the amorphous results were observed to display an "excess" heat capacity which could be accounted for by the occurrence of a single delta function peak in the low frequency part of the vibrational spectrum. This excess did not appear in the completely crystalline extrapolated data, and the specific heat was found to be proportional to the cube of the temperature up to 9°K. (U)

An attempt was made to compare the results with two theoretical models (Tarasov and Stockmayer-Hecht) with only fair agreement in one case, and none in the other. The agreement with previous experimental results is excellent if the density dependence and the excess heat capacity are considered. (U)

DD FORM 1 JAN 64 1473

14. KEY WORDS	LINK A		LINK B		LINK C	
	ROLE	WT	ROLE	WT	ROLE	WT
Heat Capacity Specific Heat Polyethylene Low Temperatures						

INSTRUCTIONS

1. ORIGINATING ACTIVITY: Enter the name and address of the contractor, subcontractor, grantee, Department of Defense activity or other organization *(corporate author)* issuing the report.

2*a*. REPORT SECURITY CLASSIFICATION: Enter the overall security classification of the report. Indicate whether "Restricted Data" is included. Marking is to be in accordance with appropriate security regulations.

2*b*. GROUP: Automatic downgrading is specified in DoD Directive 5200.10 and Armed Forces Industrial Manual. Enter the group number. Also, when applicable, show that optional markings have been used for Group 3 and Group 4 as authorized.

3. REPORT TITLE: Enter the complete report title in all capital letters. Titles in all cases should be unclassified. If a meaningful title cannot be selected without classification, show title classification in all capitals in parenthesis immediately following the title.

4. DESCRIPTIVE NOTES: If appropriate, enter the type of report, e.g., interim, progress, summary, annual, or final. Give the inclusive dates when a specific reporting period is covered.

5. AUTHOR(S): Enter the name(s) of author(s) as shown on or in the report. Enter last name, first name, middle initial. If military, show rank and branch of service. The name of the principal author is an absolute minimum requirement.

6. REPORT DATE: Enter the date of the report as day, month, year, or month, year. If more than one date appears on the report, use date of publication.

7*a*. TOTAL NUMBER OF PAGES: The total page count should follow normal pagination procedures, i.e., enter the number of pages containing information.

7*b*. NUMBER OF REFERENCES: Enter the total number of references cited in the report.

8*a*. CONTRACT OR GRANT NUMBER: If appropriate, enter the applicable number of the contract or grant under which the report was written.

8*b*, 8*c*, & 8*d*. PROJECT NUMBER: Enter the appropriate military department identification, such as project number, subproject number, system numbers, task number, etc.

9*a*. ORIGINATOR'S REPORT NUMBER(S): Enter the official report number by which the document will be identified and controlled by the originating activity. This number must be unique to this report.

9*b*. OTHER REPORT NUMBER(S): If the report has been assigned any other report numbers *(either by the originator or by the sponsor)*, also enter this number(s).

10. AVAILABILITY/LIMITATION NOTICES: Enter any limitations on further dissemination of the report, other than those imposed by security classification, using standard statements such as:

(1) "Qualified requesters may obtain copies of this report from DDC."

(2) "Foreign announcement and dissemination of this report by DDC is not authorized."

(3) "U. S. Government agencies may obtain copies of this report directly from DDC. Other qualified DDC users shall request through _____."

(4) "U. S. military agencies may obtain copies of this report directly from DDC. Other qualified users shall request through _____."

(5) "All distribution of this report is controlled. Qualified DDC users shall request through _____."

If the report has been furnished to the Office of Technical Services, Department of Commerce, for sale to the public, indicate this fact and enter the price, if known.

11. SUPPLEMENTARY NOTES: Use for additional explanatory notes.

12. SPONSORING MILITARY ACTIVITY: Enter the name of the departmental project office or laboratory sponsoring *(paying for)* the research and development. Include address.

13. ABSTRACT: Enter an abstract giving a brief and factual summary of the document indicative of the report, even though it may also appear elsewhere in the body of the technical report. If additional space is required, a continuation sheet shall be attached.

It is highly desirable that the abstract of classified reports be unclassified. Each paragraph of the abstract shall end with an indication of the military security classification of the information in the paragraph, represented as *(TS), (S), (C), or (U)*.

There is no limitation on the length of the abstract. However, the suggested length is from 150 to 225 words.

14. KEY WORDS: Key words are technically meaningful terms or short phrases that characterize a report and may be used as index entries for cataloging the report. Key words must be selected so that no security classification is required. Identifiers, such as equipment model designation, trade name, military project code name, geographic location, may be used as key words but will be followed by an indication of technical context. The assignment of links, roles, and weights is optional.

DD FORM 1 JAN 64 1473 (BACK)